Environmental Ambition and Economic Protectionism: The Design of Border Carbon Adjustments

By Eunseong Park, Sebastian Rausch, and Valerie J. Karplus*

May 2026

Border carbon adjustments (BCAs) are intended to limit carbon leakage while protecting domestic industry, but governments differ over whether border charges should price total embodied emissions or only emissions above an intensity benchmark. We study this design choice in a plant-level general equilibrium model of the global steel industry with heterogeneous technologies and vertical supply chains. A rate-based BCA is equivalent to an emissions charge combined with an implicit output subsidy. It therefore weakens the carbon-price signal, encourages reshuffling of cleaner output toward the regulated market, and can induce leakage through underpriced carbon-intensive intermediates. In an EU-style setting with domestic carbon pricing, the rate-based design transmits only 36% of the mass-based border price needed to achieve the same global emissions reduction and yields larger welfare losses. In a US-style setting without a domestic carbon-price anchor, it mainly shifts rents toward domestic downstream industries rather than inducing abatement abroad. (JEL: F18, Q58, H23, L61, C63. Keywords: border carbon adjustments, carbon leakage, climate policy, steel industry, general equilibrium, vertical supply chains, emission intensity benchmarks.)

Unilateral climate policy asks governments to pursue two objectives at once. The first is environmental ambition: domestic carbon prices should induce emissions reductions even in sectors exposed to global trade. The second is economic protection: climate policy should not simply shift production, jobs, and rents toward foreign producers facing weaker regulation. Border carbon adjustments (BCAs) promise to reconcile these objectives by charging imports for the emissions embodied in traded goods, thereby limiting carbon leakage and reducing the competitive disadvantage faced by regulated domestic producers (Böhringer, Balistreri and Rutherford, 2012; Clausing and Wolfram, 2023; Fontagné and Schubert, 2023). Whether a BCA can deliver this reconciliation, however, depends on its architecture. Border instruments differ in how they price embedded emissions, how strongly they transmit domestic climate ambition abroad, and which parts of the supply chain they protect. The policy question is therefore not only whether to use a BCA, but which design to choose.

The key architectural divide in current policy debates is whether the border instrument prices absolute embodied emissions or only deviations from a benchmark. A mass-based BCA prices the total embodied emissions in an imported good. The European Union's

* Park (eunseong.park@zew.de): ZEW-Leibniz Centre for European Economic Research, Mannheim, Germany, and University of Mannheim, Germany. Rausch (sebastian.rausch@zew.de): Department of Economics, Heidelberg University, Heidelberg, Germany, ZEW-Leibniz Centre for European Economic Research, Mannheim, Germany, Centre for Energy Policy and Economics at ETH Zurich, Zurich, Switzerland, and Joint Program on the Science and Policy of Global Change at MIT, Cambridge, USA. Karplus (vkarplus@andrew.cmu.edu): Department of Engineering and Public Policy, Carnegie Mellon University, Pittsburgh, USA, MIT Energy Initiative and MIT Center for Energy and Environmental Policy Research, Cambridge, USA. We are grateful for helpful comments and suggestions to Christoph Böhringer, Gustav Fredriksson, Robin Sogalla, Sabine Stillger, Ulrich Wagner, as well as participants at AERE 2025 Summer Conference, EAERE Annual Conference 2025, and VfS Annual Conference 2025 for their helpful discussions and feedback. The authors acknowledge funding from the German Federal Ministry of Research, Technology and Space under the ARIADNE project. This material is based upon work supported by the National Science Foundation under Grant No. OISE 2230743.

Carbon Border Adjustment Mechanism (CBAM) follows this logic.[1] A rate-based BCA instead prices the difference between an importer's emissions intensity and a benchmark. This logic appears in recent US policy discussions: the PROVE IT Act would create product-level emissions-intensity data infrastructure, while the Foreign Pollution Fee Act would impose import fees linked to foreign pollution intensity.[2] The distinction is economically important. A mass-based BCA works like a carbon tariff on each unit of embodied emissions. A rate-based BCA combines a tax on emissions with a credit for output up to the benchmark, making it a performance standard rather than a pure carbon price (Fischer and Fox, 2012; Holland, 2012).

We show that choosing between these architectures forces the government or regulator to take a stance on the relative weight placed on environmental ambition and economic protection. Mass-based BCAs preserve more of the carbon price signal and provide stronger protection to upstream domestic producers, but they pass larger cost increases to downstream users. Rate-based BCAs cushion downstream prices, but they dilute the carbon signal faced by foreign producers and weaken protection for the domestic upstream industry. These trade-offs organize the paper's central questions: how much of a nominal carbon price does each BCA design transmit to foreign producers; how does the design allocate protection between upstream producers and downstream users; and how do these choices affect welfare, leakage, and global emissions with and without a domestic carbon price?

We analyze these trade-offs in the global steel industry, a key energy-intensive and trade-exposed (EITE) sector. Steel is responsible for roughly 7 percent of global greenhouse gas emissions, is heavily traded, and is central to current BCA policy debates (World Steel Association, 2023). It is also one of the hard-to-abate sectors most tightly integrated into the production and consumption activities that underpin economic activity. Steel is used in construction, transportation, machinery, and energy infrastructure; it was foundational to past industrial development and is central to future decarbonization. This makes steel an important test bed for designing effective and efficient climate-trade policy for EITE sectors, where governments want to preserve industrial competitiveness while inducing emissions reductions across global supply chains.

Steel is a natural setting for studying BCA design because both margins on which design matters are economically large. First, high trade exposure combined with large differences in plant technologies creates substantial scope for carbon leakage through reshuffling. Exporters can reallocate cleaner output toward regulated markets while diverting dirtier output elsewhere, especially because emissions intensities differ sharply between integrated blast furnace-basic oxygen furnace (BF-BOF) production and scrap-based electric arc furnace (EAF) production (Mathiesen and Mæstad, 2004; Collard-Wexler and De Loecker, 2015; Duscha et al., 2019; Cohen and Valacchi, 2022). Second, steel has rich vertical linkages. Carbon-intensive iron can be produced on site, embedded in finished steel, or traded separately through merchant markets for pig iron and direct reduced iron (DRI). This gives downstream firms a second response margin: when border charges do not fully follow emissions through the supply chain, they can substitute toward unregulated or underpriced carbon-intensive intermediates.

The analysis proceeds in two steps. We first develop a stylized equilibrium framework that makes the design trade-off transparent. The key insight is that a rate-based BCA

[1] The EU CBAM started on January 1, 2026. Initial coverage includes cement, iron and steel, aluminium, fertilizers, electricity, and hydrogen; importers surrender CBAM certificates linked to EU ETS allowance prices, with deductions for carbon prices already paid abroad.

[2] The PROVE IT Act of 2024 (S.1863, 118th Congress) would estimate average product emissions intensities for covered goods produced in the US and selected foreign countries; it does not itself impose a border charge. The Foreign Pollution Fee Act of 2025 (S.1325, 119th Congress) would impose an ad valorem fee on covered imported products based on pollution-intensity differences relative to a baseline. Covered categories include aluminium, cement, iron and steel, fertilizers, glass, hydrogen, solar products, and battery inputs.

is not simply a weaker mass-based BCA. By charging emissions relative to a benchmark, it combines a carbon charge with an implicit output subsidy. We summarize this wedge with the effective signal ratio: the share of the nominal carbon price actually transmitted to foreign producers at the border. The theory then links this wedge to the paper's main mechanisms and quantitative results. Because the benchmark mutes the scale margin, a rate-based BCA is less cost-effective for a given global emissions target and shifts adjustment toward technology switching and compositional responses. With heterogeneous plants, it creates scope for reshuffling, as exporters redirect cleaner units to the regulated market. With vertically linked production and more homogeneous upstream inputs, it can also generate vertical leakage by leaving iron intermediates only weakly priced. The framework further clarifies the distributional stakes: mass-based BCAs protect upstream producers and generate fiscal revenue, whereas rate-based BCAs shield downstream users through the benchmark subsidy.

We then quantify these mechanisms in a plant-level, structurally calibrated general equilibrium model of the global steel supply chain. The model tracks roughly 300 steel mills across 48 countries in 15 regions.[3] It captures the distinct vertical pathways through which iron and steel are produced, including integrated BF-BOF production, scrap-based EAF production, and merchant iron markets for pig iron and DRI. Plants face heterogeneous local input prices and emissions intensities and choose technologies, input mixes, product composition, and whether to source iron internally or through markets. Buyers demand differentiated flat and long steel from domestic and foreign origins, while both intermediate inputs and finished products are traded bilaterally. We calibrate the model using a rich combination of industrial micro-data, bilateral trade flows and trade margins, firm-level trade statistics, and macroeconomic input-output and national accounting data. Plant-level production responses are disciplined by engineering information on technologies, metallurgical constraints, and thermal rigidities, which is essential for credibly quantifying reshuffling, vertical leakage, welfare, and incidence under alternative BCA designs.

These design trade-offs also depend on the broader policy environment in which the border instrument operates. We therefore study two settings that map directly onto the paper's central questions. In the symmetric environment, modeled on the EU, a BCA complements a domestic carbon price, so the issue is how alternative border designs transmit an existing climate signal while allocating protection across the supply chain. In the asymmetric environment, modeled on current US policy discussions, the border measure operates without a domestic carbon-price anchor, so the question is whether a border instrument can do more than protect domestic industry. This contrast shows when the choice between mass-based and rate-based BCAs is mainly about the incidence of a given climate ambition and when it is also about whether meaningful climate ambition is transmitted abroad at all.

Our first result is that rate-based BCAs substantially dilute the effective carbon signal. In the EU-style symmetric setting, a rate-based BCA is equivalent to applying only 36 percent of the mass-based border carbon price that would deliver the same global emissions reduction. Put differently, the benchmark creates a 64 percent discount on the carbon price. This dilution is not only an accounting feature. It changes the abatement margins: relative to a mass-based BCA, the rate-based design preserves more trade volume and therefore relies more on reshuffling, technology composition, and intermediate-input responses. The same logic implies that, without a domestic carbon-price anchor, a rate-based BCA is ill-suited to induce emissions reductions abroad and instead operates primarily as

[3]This plant layer covers 55.9% of world production overall and 70.3% outside China, and its capacity distribution closely matches the comprehensive Global Steel Plant Tracker, a near-census database covering 96.1 percent of global steelmaking capacity, making it broadly representative of global production structure (Figure C1).

a rent-shifting tariff.

Second, the diluted signal has meaningful welfare and leakage consequences. At a stringency corresponding to a 30 percent reduction in EU domestic steel emissions, the mass-based BCA reduces global steel emissions by 1.34 percent. The rate-based BCA reduces global emissions by only 1.02 percent and raises EU welfare losses by about 55 percent relative to the mass-based design. The leakage rate increases from 16 percent under the mass-based design to 36 percent under the rate-based design. A major reason is revenue and incidence: the rate-based benchmark protects downstream users from some price increases, but it forgoes fiscal revenue and leaves domestic upstream producers facing stronger import competition.

Third, vertical linkages are quantitatively important. Relative to the EU mass-based BCA, the rate-based design more than doubles pig iron imports into the EU and leaves their import price about 41 percent lower. The reason is that pig iron production is technologically more homogeneous than finished steel production. When the benchmark is set near the prevailing emissions intensity of a homogeneous upstream product, the rate-based charge can transmit little price signal at the upstream stage, encouraging downstream steelmakers to rely on imported carbon-intensive intermediates. Models that omit vertical linkages within the steel supply chain miss this channel.

Fourth, standalone BCAs have limited leverage over global emissions. In the US-style asymmetric setting, the rate-based design delivers only about one-quarter of the global emissions reduction achieved by the corresponding mass-based import charge at the same reference carbon price. With the mass-based benchmark normalized to an effective signal ratio of 1, the rate-based standalone instrument falls to about 0.12 and thus transmits only about one-eighth of the corresponding carbon-price signal. More broadly, even the mass-based standalone instrument has limited leverage without a domestic carbon-price anchor. Such instruments can protect domestic output and shift production toward the US, but without domestic carbon pricing they provide weak incentives for global decarbonization.

These findings have three implications for climate-trade policy. First, BCA design and domestic carbon pricing are complements. Border measures can extend a domestic carbon price, but they are poor substitutes for one, especially when a standalone rate-based instrument mainly shifts rents rather than inducing abatement abroad. Second, benchmark design, including the treatment of intermediate inputs, matters for environmental performance. Benchmarks that protect downstream users can undermine effectiveness when they mute the scale margin, encourage reshuffling, or leave homogeneous upstream inputs underpriced; this logic extends beyond steel to other energy-intensive, trade-exposed sectors with technological heterogeneity and vertical supply chains. Third, evaluating BCAs requires a model that tracks heterogeneity within industries and vertical linkages across production stages. In steel, reshuffling and upstream leakage are the channels through which BCA design shapes both the incidence of the policy and the amount of global abatement it delivers. To the extent that other EITE sectors share these features, our analysis carries broader implications for BCA design beyond steel.

This paper departs from existing work in several ways. First, to our knowledge, it is the first economic analysis to center a fundamental BCA design choice with first-order implications for the balance between environmental ambition and economic protection: whether the border instrument prices the full embodied emissions content of imports or only emissions above a benchmark. This mirrors the classic domestic climate-policy question of whether to regulate emissions with a market-based price instrument or with an intensity standard or clean-energy quota (Fullerton and Metcalf, 2001; Holland, Hughes and Knittel, 2009; Holland, 2012; Goulder, Hafstead and Williams III, 2016; Abrell, Rausch and Streitberger, 2019). At the border, these correspond to a mass-based tariff and a rate-based benchmark instrument, the latter combining an emissions charge with an implicit

subsidy to import volume. While that literature studies the price-versus-standard trade-off within the regulated jurisdiction, the economics literature on BCAs has, to our knowledge, not analyzed this border-design choice as a central question.

Second, a growing literature studies how unilateral climate policy, border adjustments, and climate clubs can address free riding, shift rents, limit leakage, and improve global incentives (Copeland, 1996; Keen and Kotsogiannis, 2014; Nordhaus, 2015; Weisbach et al., 2023; Beaufils, Wanner and Wenz, 2024; Farrokhi and Lashkaripour, 2025; Itskhoki and Mukhin, 2025; Keen and Kotsogiannis, 2025; Kortum and Weisbach, 2026). Within this literature, analyses of BCA design mostly focus on whether border adjustment should be import-only or combined with export rebates, how broad sectoral coverage should be, how embodied emissions should be measured or benchmarked, and how BCAs can be adapted to domestic policies that rely on partial pricing or nonprice regulation rather than a full domestic carbon price (Fischer and Fox, 2012; Fowlie, Petersen and Reguant, 2021; Pizer and Campbell, 2021; Campolmi et al., 2025; Clausing and Wolfram, 2023; Clausing et al., 2025). We show that, beyond the decision to use a border measure at all, the choice between mass- and rate-based border architecture is itself first-order because it determines how much of the nominal carbon price is transmitted and where protection is allocated within the supply chain.

Third, we contribute to work on carbon leakage and trade responses to environmental regulation (Copeland and Taylor, 2004; Felbermayr, Peterson and Wanner, 2025; Fontagné and Schubert, 2023). Earlier retrospective studies often find limited production relocation under initial carbon-pricing regimes (Dechezleprêtre et al., 2022; Akerman, Forslid and Prane, 2024), while recent firm-level evidence points to supply-chain adjustment and carbon offshoring (Ben-David et al., 2021; Coster, Mejean and di Giovanni, 2024). Our results help reconcile these findings by showing that leakage in hard-to-abate sectors can occur through intermediate inputs and within-industry reallocation, margins that are difficult to detect in aggregate sectoral data and modelling.

Fourth, we extend environmental trade models with firm and plant heterogeneity (Shapiro and Walker, 2018; Sogalla, Wanner and Watabe, 2024; Sogalla, 2025). Existing work has used plant-level data to study incidence and reallocation under environmental policy (Clausing et al., 2025; Stillger, 2025). We combine plant-level heterogeneity with explicit vertical linkages in a multi-region general equilibrium model, allowing us to quantify reshuffling and vertical leakage under alternative BCA architectures.

We proceed as follows. Section I describes the global steel industry and its vertical structure. Section II develops the conceptual framework. Section III presents the quantitative model. Section IV describes the data and calibration. Section V first lays out the design of the counterfactual experiments and then presents the model-based estimates. Section VI concludes.

I. Industry Background

This section describes the features of the steel industry that are central to the paper's analysis of BCA design. Steel is a natural setting in which to study this question because the margins emphasized in the paper—heterogeneity in embodied emissions and vertical linkages—are both economically important in this sector. The purpose is not to provide a general primer on steelmaking, but to isolate the features that determine how border instruments transmit climate ambition abroad, create scope for reshuffling and vertical leakage, and allocate protection across the supply chain in the quantitative analysis that follows.

Two features are central. First, steel production is technologically heterogeneous, meaning otherwise similar products embody very different emissions and production costs across plants. Second, steel is produced in a vertically linked chain in which carbon-intensive

intermediates such as pig iron and DRI can be traded separately from finished steel. Together, these features explain why the choice between mass-based and rate-based BCAs has first-order consequences in steel.

A. Production Routes, Emissions, and Costs

Steel is produced through several routes with distinct input bundles and emissions intensities. The dominant integrated route (BF-BOF) accounts for about 70% of global production (World Steel Association, 2022). It uses iron ore and coke to produce hot metal in a blast furnace, and then refines that metal into crude steel in a basic oxygen furnace. This route is structurally rigid and carbon intensive, averaging roughly 2.36 tonnes of CO_2 per tonne of crude steel.[4] Its high emissions are driven by the ironmaking stage, where coal accounts for nearly 88.7% of energy costs. Furthermore, it is thermally integrated: keeping iron molten saves substantial energy, so steel shops rely almost universally on on-site, captive iron (averaging over 96.2% of their iron charge) rather than merchant markets. Finally, while BOF plants can add scrap to lower emissions, metallurgical and thermal constraints tightly constrain this scrap addition to an average of about 11.7%.

EAF production accounts for the remaining 30% of world output and can be much less emissions intensive when it relies on scrap and relatively clean electricity. In the US, where scrap availability is high and electricity prices have historically favored EAFs, this route accounts for around 70% of production. The EAF route offers substantial flexibility in its metallic charge, with scrap shares averaging roughly 73.4%. However, global scrap supply is limited by the long service life of steel products, and its quality is often insufficient for advanced steel grades. Consequently, many EAF producers cannot operate on scrap alone and must blend it with purer, carbon-intensive primary iron units such as pig iron or DRI. The DRI-EAF route, which is common in regions with abundant natural gas, averages roughly 1.4 tonnes of CO_2 per tonne of steel, while scrap-intensive EAF production can be as low as about 0.3 tonnes when electricity is clean.[5]

Figure 1 illustrates the geographic clustering of these production technologies. With the exception of China, long products are mainly produced by EAF mills, whereas flat products are predominantly produced by BF-BOF plants, though regions such as the US, India, and some Western Asian producers maintain substantial EAF shares. As Figure 2 demonstrates, this geographic clustering translates into massive dispersion in plant-level unit costs and emissions intensities. The global supply curve for steel is not uniform but exhibits substantial heterogeneity in both costs and emissions, reflecting the physical realities of the global fleet: differences in local ore quality, regional energy grids, and the vintage of the capital stock.

This dispersion is the exact structural condition required for carbon reshuffling. When the same steel product can embody very different carbon content and baseline costs across plants, the choice between pricing all embedded emissions and pricing only emissions above a benchmark has large consequences. While any carbon border charge incentivizes foreign regions to shuffle their cleanest output to the regulated market, a rate-based BCA amplifies this effect. Because it only taxes the deviation from a benchmark, it creates an implicit output subsidy that preserves overall trade volumes. This forces exporters to rely more heavily on diverting their existing clean production (e.g., EAFs) to the regulating region rather than reducing total emissions, deepening the gap between apparent clean imports and actual global abatement.

[4] Unless otherwise noted, industry statistics in this section are derived from the global plant-level dataset provided by the CRU Steel Cost Service. Detailed summary statistics and sample coverage are provided in Table 1 in Section IV.

[5] While our sample average for the EAF route is 0.62 tCO_2/t, the variance is large and heavily dependent on the local electricity grid and the specific metallic charge used.

(a) Flat Steel (b) Long Steel

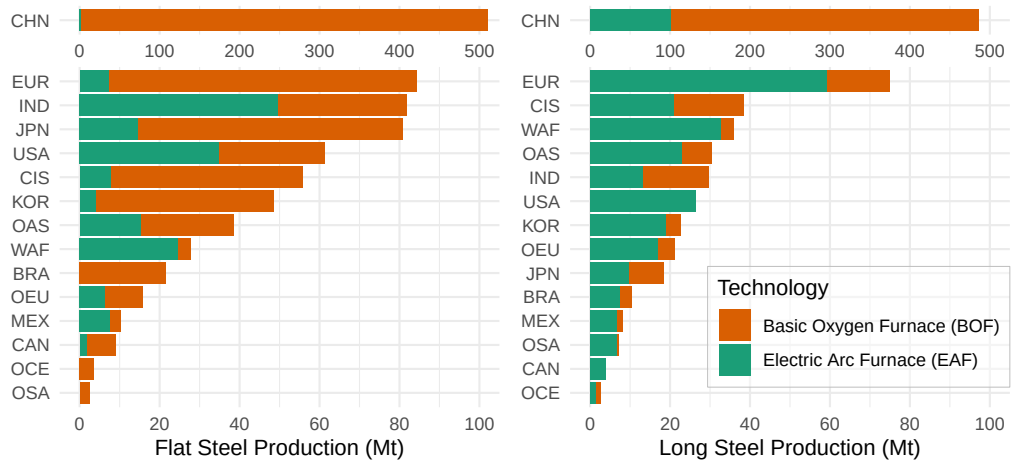

Figure 1. Steel Production by Technology and Region

Notes: Bars report production by region, with fill indicating technology (BOF vs. EAF); production is in Mt. Region codes: EU28/EFTA (EUR), US (USA), China (CHN), India (IND), Japan (JPN), South Korea (KOR), Other Asia (OAS), Oceania (OCE), Canada (CAN), Mexico (MEX), Brazil (BRA), Other South America (OSA), Turkey and Other Europe (OEU), CIS and Ukraine (CIS), and Western Asia and Africa (WAF). Source: Own calculations based on CRU Group (2023) and World Steel Association (2022).

(a) Emissions Intensity (b) Unit Cost

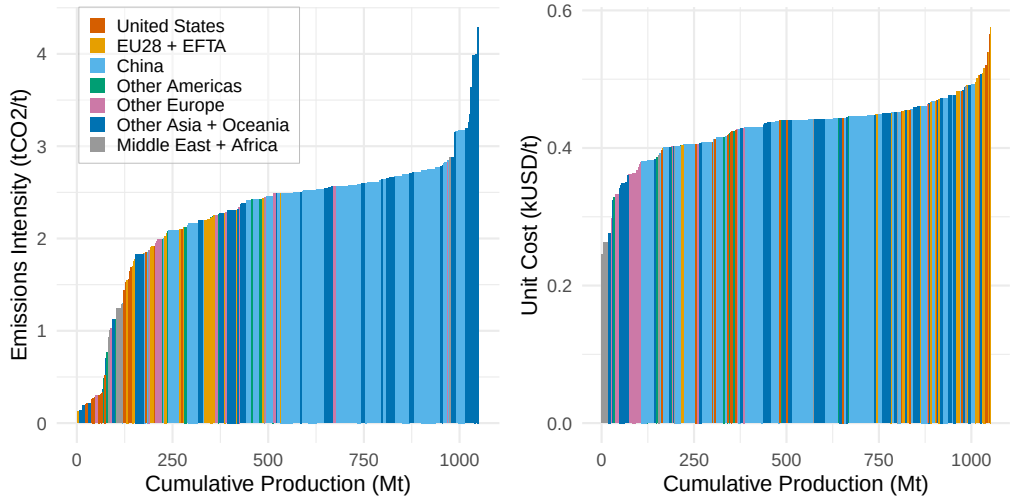

Figure 2. Cost and Emissions Intensity Curve for Flat Steel

Notes: Each panel plots flat-steel plants ordered by cumulative production. Bars are colored by region code (see legend), bar width equals plant production, and cumulative production is in Mt. The left panel reports emissions intensity (tCO_2/t) and the right panel reports unit cost (USD/t). Source: Own calculations based on CRU Group (2023) and World Steel Association (2022).

B. Vertical Linkages and Asymmetric Integration

Steel has traditionally been a vertically integrated industry, but this integration is highly asymmetric across technologies. In the dominant BF-BOF route, iron is almost universally produced on site and transferred internally as hot metal. This reliance on captive iron

(averaging over 96.2% of the iron charge) means integrated producers are structurally committed to their own ironmaking.

In contrast, the secondary EAF route relies heavily on merchant markets, with captive iron averaging only 21.5% of the iron charge. EAF producers frequently blend scrap with primary iron units—most importantly pig iron and DRI—purchased from third parties to meet purity requirements. This asymmetry creates a distinct trade margin for intermediates. This vertical structure is the second reason BCA design matters in our analysis. A border measure that weakly prices upstream carbon, or that benchmarks it against a relatively homogeneous intermediate, can leave much of the carbon cost outside the effective policy base. In that case, the instrument may still cushion downstream steel users, but it does so partly by shifting protection away from upstream producers and by encouraging flexible downstream producers to substitute toward underpriced imported intermediates. This creates a structural opening for vertical leakage that is a direct consequence of the industry's asymmetric integration.

Taken together, these industry features dictate our modeling strategy in Section III. Plant-level heterogeneity is needed to capture how alternative border designs interact with wide dispersion in embodied emissions and baseline costs to drive reshuffling. Explicit merchant iron markets are needed to quantify substitution toward upstream intermediates and the resulting vertical leakage. A general-equilibrium framework is needed to track how these instruments reallocate protection across upstream producers, downstream users, and foreign suppliers.

II. Theory and Mechanisms

This section develops a stylized theory framework that isolates the economic architecture behind the paper's central design question: what changes when the border instrument prices all embodied emissions versus only emissions above a benchmark. The framework is not meant to capture the full richness of the steel industry. Its role is to make transparent how a rate-based benchmark dilutes the carbon-price signal, shifts adjustment toward reshuffling and technology composition, and reallocates protection across the supply chain. In this way, the theory provides a roadmap for the quantitative results that follow. Appendix A contains the proofs for all lemmas and propositions.

A. Setup

To isolate the margins emphasized in the introduction, we consider a vertically linked economy with two sectors: an upstream sector and a domestic downstream sector. The upstream sector spans two regions home (h) and foreign (f): $i \in \{h, f\}$. To capture the range of policy environments relevant for BCA design, we distinguish between the domestic carbon price $\tau_h \geq 0$ faced by home producers and the border adjustment rate $\tau_f > 0$ applied to imports from the foreign region. This setup nests both the symmetric paradigm ($\tau_h = \tau_f$, modeled on the EU) and the asymmetric paradigm ($\tau_h = 0$, modeled on the US). Throughout the framework, we assume perfect competition at the plant level. This ensures that plants act as price-takers, allowing us to cleanly isolate the policy-driven margins of technology substitution and trade reshuffling. Allowing these two policy wedges to vary separately lets the framework distinguish between a border measure that extends domestic climate ambition and one that operates without a domestic price anchor.

UPSTREAM SECTOR.—Each regional upstream sector is characterized by a representative producer managing a portfolio of clean (c) and dirty (d) technologies with emissions intensities $\epsilon_c < \epsilon_d$ and base unit production costs $c_c > c_d$. The producer's sectoral unit cost of production $c(s_{c,i})$ depends on the regional aggregate clean technology share $s_{c,i} \in [0, 1]$ and is strictly increasing and convex ($c' > 0, c'' > 0$), reflecting the weighted average

of base technology costs and the increasing marginal costs of technology integration and site-specific constraints.

Home upstream producers supply volume $q_{h,h}$ exclusively to the regulated domestic market, while foreign upstream producers serve both the regulated market ($q_{f,h}$) and an unregulated foreign domestic market ($q_{f,f}$). We consider inelastic foreign domestic demand $q_{f,f}$ to isolate the policy-driven trade-offs between technology adoption and trade scale within the regulated market. Let $\omega_{i,j} = q_{i,j}/(q_{i,h} + q_{i,f})$ denote the share of destination $j \in \{h, f\}$ in the total production of region i, where $\omega_{h,h} = 1$ and $\omega_{h,f} = 0$. The border charge $t(\cdot)$ applies only to the volume sold in the regulated market ($j = h$) based on its specific intensity $\epsilon_{i,h} = s_{c,i,h}\epsilon_c + (1 - s_{c,i,h})\epsilon_d$. The representative producer in region i chooses the clean technology shares for each market ($s_{c,i,h}, s_{c,i,f}$) to minimize the unit cost of the variety sold in the regulated market:

$$\min_{s_{c,i,h}, s_{c,i,f}} \{c(s_{c,i}) + t(\epsilon_{i,h})\} \tag{1}$$

where $s_{c,i} = \sum_j \omega_{i,j} s_{c,i,j}$ is the regional clean share. The instrument $t(\epsilon)$ is determined by the policy design: $t^M(\epsilon) = \tau\epsilon$ under a mass-based design, and $t^R(\epsilon) = \tau(\epsilon - \bar{\psi})$ under a rate-based design, where $\bar{\psi}$ denotes the intensity benchmark. Economically, the rate-based design is equivalent to a mass-based tax combined with a specific output subsidy $\tau\bar{\psi}$. In equilibrium, the price $p_{i,h}$ of the regional variety in the regulated market is $p_{i,h} = c(s_{c,i}) + t(\epsilon_{i,h})$.

DOWNSTREAM SECTOR.—Domestic downstream firms combine domestic ($q_{h,h}$) and foreign ($q_{f,h}$) upstream varieties to produce a composite intermediate Q. The aggregation follows a linearly homogeneous and concave function $Q = F(q_{h,h}, q_{f,h})$. Let $P(p_{h,h}, p_{f,h})$ denote the associated dual price index, representing the minimum cost of producing one unit of Q. This index is strictly increasing ($\partial P/\partial p_{i,h} > 0$) and concave ($\partial^2 P/\partial p_{i,h}^2 \leq 0$) in input prices. Downstream firms choose Q to maximize producer surplus $\Pi_d = \max_Q\{G(Q) - P(p_{h,h}, p_{f,h})Q\}$, where $G(Q)$ represents the value-added of the upstream input in downstream production. By Shephard's Lemma, the demand for each variety is given by $q_{i,h} = Q \cdot \partial P/\partial p_{i,h}$. The concavity of P ensures that demand for each variety is strictly decreasing in its own price $p_{i,h}$. This downstream block is intentionally parsimonious: its role is to map border-induced changes in upstream prices into trade volumes, supply-chain incidence, and the allocation of protection between upstream producers and downstream users. This general structure can be specialized to a Constant Elasticity of Substitution (CES) functional form, consistent with standard Armington trade assumptions.

The key economic distinction between the two architectures is the benchmark credit embedded in the rate-based design. Rather than acting as a pure carbon price, the rate-based instrument combines a tax on emissions with a specific subsidy to output. The next lemma formalizes the resulting ranking of equilibrium prices and introduces the effective signal ratio that organizes the rest of the section.

LEMMA 1 (Price Ranking and Signal Dilution): *The equilibrium price under a rate-based design is strictly lower than under a mass-based design subject to the same statutory carbon price τ: $p_{i,h}^R < p_{i,h}^M$. Let $\lambda = (1 - \bar{\psi}/\epsilon_{i,h})$ denote the effective signal ratio. The effective carbon price faced by imports under a rate-based design is $t^R = \lambda\tau\epsilon_{i,h}$, where $\lambda < 1$ represents the inherent dilution of the carbon signal created by the intensity benchmark.*

This price wedge means that a rate-based BCA transmits only a fraction of the nominal carbon price to foreign producers at the border. By lowering the effective border price relative to the nominal carbon price, the benchmark does not merely weaken stringency in a uniform way; it changes which margins absorb a given emissions target. In the

symmetric setting, this means weaker transmission of domestic climate ambition abroad. In the asymmetric setting, it foreshadows why a standalone benchmarked instrument can look more like a rent-shifting tariff than a climate policy.

B. Signal Transmission and Global Cost-Effectiveness

To compare the two designs on common ground, we hold global emissions fixed and ask which instrument achieves a given target at lower cost. A nominal border price is not a sufficient metric for this comparison, because the benchmark changes how much of that price is actually transmitted. The object λ, the *effective signal ratio*, captures this distinction by measuring the fraction of the full carbon cost that is applied at the border.

PROPOSITION 1 (Global Cost-Effectiveness): *For a fixed global emissions target $\bar{E}$, the mass-based BCA is strictly more cost-effective than the rate-based BCA. The rate-based design induces a distorted allocation of abatement by neutralizing the consumption margin, forcing all abatement onto the technology margin where marginal costs are increasing and convex.*

This proposition establishes the first building block of the paper. Because the benchmark credit mutes the scale margin, the rate-based design forces a larger share of adjustment onto technology upgrading and composition. The same nominal border price therefore does not represent the same climate signal under the two architectures, and the rate-based design is strictly less cost-effective once the comparison is made at a common global emissions target.

C. Abatement Margins and Reshuffling

The efficiency gap immediately implies a different mix of abatement channels. The relevant question is not only how much abatement occurs, but whether it comes from lower trade volume, cleaner production, or reallocation of existing clean units toward the regulated market. These are the margins behind the paper's reshuffling results.

PROPOSITION 2 (Foreign Composition–Scale Substitution): *Consider a comparison between a rate-based design and a mass-based design achieving the same global emissions reductions. For a fixed domestic emissions target, the rate-based design induces a strictly larger compositional shift in the foreign sector (higher $s_{c,f}$). Because the rate-based design preserves trade volumes more effectively than a mass-based design of equivalent stringency, it must compensate with a deeper reduction in the technological composition of production to satisfy the global emissions budget.*

For a common emissions target, the rate-based design preserves more trade volume and therefore must deliver more abatement through composition. This is the formal counterpart to the diluted-signal logic in the introduction: once the scale margin is muted, exporters are pushed toward cleaner average export bundles rather than lower exports. For multi-plant producers, the first and least costly way to do this is often to redirect already-clean units toward the regulated market.

LEMMA 2 (Reshuffling Priority): *Foreign producers will always prioritize the allocation of upstream production from clean technology plants to the regulated market to minimize the border charge. This priority rule holds whenever the carbon price makes the tax savings from the intensity gap outweigh the costs of technology integration.*

This priority rule shows why reshuffling is a central challenge for benchmarked border measures. Producers will first exhaust their cleanest units in serving the regulated market

whenever the tax savings from doing so exceed the cost of reorganizing production. But the scope for this margin depends on trade scale. If export volume remains high, the existing stock of clean capacity may be insufficient to meet the benchmark for all shipments, making reshuffling progressively more costly.

PROPOSITION 3 (Reshuffling and Capacity Pressure): *For a fixed import emissions intensity target $\bar{\psi}_{f,h}$, the rate-based BCA drives a larger expansion of clean technology capacity in the foreign sector. Because the rate-based design sustains higher export volumes $q_{f,h}$, satisfying the intensity constraint at the border requires a larger absolute quantity of clean production, which exceeds the reshuffling potential of the baseline technology mix.*

This proposition makes clear that reshuffling and real abatement are linked by volume. Because the rate-based design sustains higher exports, it eventually pushes exporters beyond what can be achieved by simple reallocation of clean units. At that point, the benchmark forces genuine technology switching. The theory thus rationalizes why a diluted border signal can coexist with more reshuffling pressure and deeper compositional responses.

D. Protection, Incidence, and Leakage

The same benchmark subsidy that dilutes signal transmission also reallocates rents. This subsection links instrument design to the paper's second central theme: where protection is allocated within the supply chain, and how that allocation shapes leakage incentives. We begin with the regional incidence of the two designs.

PROPOSITION 4 (Regional Incidence and Terms-of-Trade): *The choice of BCA design determines the distribution of economic surplus between regions. For a fixed marginal carbon price τ_f, the mass-based design improves the Home region's terms-of-trade by capturing scarcity rents from foreign producers, while the rate-based design foregoes this fiscal revenue to minimize downstream costs.*

The incidence decomposition makes precise why the architectural choice is also a choice about economic protection. A mass-based design converts part of the scarcity rent created by the border measure into public revenue and stronger protection for domestic upstream production. A rate-based design instead returns part of those rents to downstream users through lower input prices.

PROPOSITION 5 (Industrial Incidence): *The choice of BCA design determines the distribution of economic surplus between the upstream sectors and the domestic downstream sector:*

(i) Upstream: Mass-based designs maximize the competitive shield for domestic producers by increasing import prices $p_{f,h}$, thereby increasing their producer surplus: $\Pi_{u,h}(p^M_{f,h}) > \Pi_{u,h}(p^R_{f,h})$.

(ii) Downstream: Rate-based designs minimize the input price index $P(p_{h,h}, p_{f,h})$, thereby increasing the surplus of downstream firms: $\Pi_d(P^R) > \Pi_d(P^M)$.

These incidence results sharpen the tension between environmental ambition and economic protection emphasized in the introduction. Shielding downstream users by muting the border charge is not neutral: it weakens the effective carbon signal and narrows the protection afforded to domestic upstream producers. In the asymmetric setting, where no domestic carbon price anchors the policy, the same logic helps explain why the border measure can primarily reshuffle rents and production.

PROPOSITION 6 (Reshoring and Diluted Abatement): *In the asymmetric paradigm ($\tau_h = 0, \tau_f > 0$), the BCA induces reshoring of domestic production. The net impact on global emissions is determined by the trade-off between the abatement effect in the foreign sector and the substitution effect toward dirtier domestic varieties. Global emissions reductions are diluted if the reshoring of unabated domestic production is large relative to the technology response of foreign producers.*

Up to this point, the upstream sector has been treated as a single stage. To connect the framework back to the industry background, we now ask how the same logic changes in a vertically linked production chain where upstream intermediates may be much more technologically homogeneous than finished steel. Because blast furnace ironmaking relies on a strict minimum of carbon (coke) as a chemical reductant, these metallurgical limits cluster upstream emissions intensities tightly together. This is exactly the setting in which benchmarking can become especially fragile.

LEMMA 3 (Homogeneous Sectors): *In a rate-based BCA, the implicit penalty δ^R becomes infinitely sensitive to the benchmark level $\bar{\psi}$ as the technology-specific emissions intensities ϵ_c and ϵ_d converge. For a sufficiently homogeneous sector ($\epsilon_c \to \epsilon_d$), any benchmark set below the physical limit of the technology leads to widespread compliance failure driving the penalty to its maximum ($\delta^R \to \infty$), while any benchmark set above it neutralizes the price signal ($\delta^R \to 0$).*

This knife-edge property is the formal reason benchmarking performs poorly in relatively homogeneous upstream segments. When emissions intensities cluster tightly, the benchmark either binds hardly at all or becomes infeasible; in either case, it fails to provide a stable carbon-price signal. The next proposition shows how this weak pricing of intermediates translates into vertical leakage.

PROPOSITION 7 (Vertical Leakage): *Consider a multi-stage production where an intermediate input is technologically homogeneous ($\epsilon_c \approx \epsilon_d \approx \bar{\psi}$). A rate-based BCA applied to the intermediate induces vertical leakage. Domestic producers of the intermediate face the full cost of domestic carbon pricing τ_h, while foreign producers face a near-zero effective border tax. This price wedge incentivizes downstream firms to substitute domestic intermediates with imports, shifting the carbon-intensive stage of production offshore.*

This final result links the conceptual framework directly to the steel application. If benchmarking is applied to an upstream intermediate with little technological heterogeneity, the rate-based design can leave imports only weakly priced and thereby encourage substitution toward foreign intermediates. Vertical leakage is therefore not an incidental feature of the steel model; it is a consequence of benchmarked border design in sectors with vertical linkages and limited upstream dispersion. Taken together, the results trace a single causal chain: the benchmark creates an implicit output subsidy, the subsidy dilutes signal transmission, and that dilution governs both the environmental performance of the policy and the allocation of protection that we quantify in the plant-level model.

III. Quantitative Model

This section translates the industry features in Section I and the mechanisms in Section II into a quantitative-empirical framework. The model is designed to quantify how alternative BCA architectures transmit carbon prices through a steel industry with plant-level heterogeneity, vertical linkages, and international trade.

OVERVIEW.—We develop a multi-region general equilibrium model of the global steel supply chain, with its high-level structural linkages illustrated in Figure 3. The framework connects regional households, which supply labor, capital, and raw materials, to a

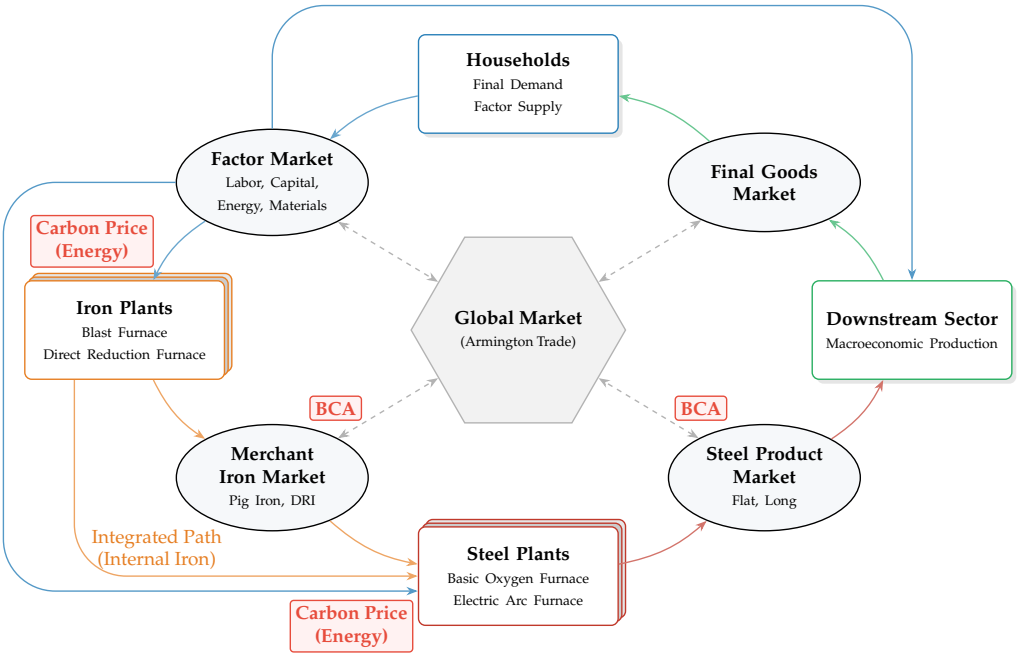

Figure 3. Model schematic.

macroeconomic production block that bundles steel, energy, and other intermediates into final consumption goods. Its distinctive feature is a granular industrial layer: individual iron and steel plants operate different technologies, face plant-specific costs and emissions intensities, and supply differentiated products to domestic and foreign markets. The model also captures the industry's vertical structure by allowing iron to be produced on-site and fed directly into steelmaking or purchased across borders through the merchant iron market.

As summarized in the schematic, the model endogenizes several key economic decisions. Plants choose input mixes, output composition, and whether to rely on integrated iron or merchant intermediates; buyers in each region choose among domestic and foreign varieties through Armington trade nests; and the macro block determines derived demand for steel. Climate-trade policy enters through regional carbon pricing on production inputs and BCAs on the embodied carbon content of imports, implemented either on a mass basis or relative to an intensity benchmark. Revenues are rebated to households, and equilibrium prices and quantities are determined jointly across factor markets, product markets, intermediate-input markets, and international trade. This structure lets us quantify signal transmission, reshuffling, vertical leakage, and the distribution of rents across upstream producers, downstream users, and foreign suppliers.

The exposition begins with the steel and ironmaking industrial layer. It then links plant-level output to regional and international markets, introduces climate policy, and closes the model with an aggregate resource constraint, households, and equilibrium conditions.

A. The Industrial Layer: Iron and Steelmaking

PLANTS, TECHNOLOGIES, AND VARIETIES.—The iron and steel sector is composed of a set of individual production facilities $i \in \mathcal{I}$. Each plant i operates a portfolio of available technologies $a \in \mathcal{A}_i \subseteq \mathcal{A}$. We explicitly partition the metallurgical supply chain into ironmaking and steelmaking stages: $\mathcal{A} = \mathcal{A}_I \cup \mathcal{A}_S$, where $\mathcal{A}_I = \{\text{blast furnace (BF)}, \text{direct reduction furnace (DRF)}\}$ and $\mathcal{A}_S = \{\text{basic oxygen furnace (BOF)}, \text{electric arc furnace (EAF)}\}$. The corresponding outputs are partitioned into intermediate iron varieties

$v \in \mathcal{V}_I = \{\text{pig iron, direct reduced iron (DRI)}\}$ and finished steel varieties $v \in \mathcal{V}_S = \{\text{flat, long}\}$. Plants act as price-takers under perfect competition, with their output levels determined by site-specific marginal costs.[6] This granular representation allows the model to capture substitution both within specific technologies (the technique margin) and across different technologies or plants (the composition margin). Furthermore, the distinction between upstream intermediates and finished steel provides the structural basis for analyzing vertical leakage through merchant iron markets.

PRIMARY PRODUCTION AND UNIT COSTS.—Production at the plant level is governed by a multi-tier nested CES cost structure. This formulation captures the hard-to-abate character of steel production by enforcing the physical limits of metallurgy while allowing for price-induced substitution across energy, capital, labor, and materials. At the plant level i using technology $a \in \mathcal{A}$, producers combine a material composite with a capital-labor-energy (KLE) bundle to produce semi-finished iron or steel. Under the assumption of perfect competition and constant returns to scale,[7] the producer price of semi-finished products is equal to its unit cost $c_{i,a}(\boldsymbol{\omega}_{i,a,f}, p_{i,a,e})$. The top-level unit cost is defined as:

$$c_{i,a} = \left[\theta_{i,a}^{\text{Mat}}(p_{i,a}^{\text{Mat}})^{1-\sigma_a} + (1-\theta_{i,a}^{\text{Mat}})(p_{i,a}^{\text{KLE}})^{1-\sigma_a}\right]^{\frac{1}{1-\sigma_a}} \tag{2}$$

where $p_{i,a}^{\text{Mat}}$ is the price of the material composite, $p_{i,a}^{\text{KLE}}$ is the cost of the KLE bundle, $\theta_{i,a}^{\text{Mat}}$ is the reference material value share, and σ_a is the top-level elasticity of substitution, calibrated to a near-Leontief value to reflect metallurgical mass balance. The cost of the KLE bundle, $p_{i,a}^{\text{KLE}}$, aggregates value-added and energy:

$$p_{i,a}^{\text{KLE}} = \left[\theta_{i,a}^{\text{VA}}(p_{i,a}^{\text{VA}})^{1-\sigma_a^{\text{KLE}}} + (1-\theta_{i,a}^{\text{VA}})(p_{i,a}^{\text{Ene}})^{1-\sigma_a^{\text{KLE}}}\right]^{\frac{1}{1-\sigma_a^{\text{KLE}}}} \tag{3}$$

where $p_{i,a}^{\text{VA}}$ is the value-added cost, $p_{i,a}^{\text{Ene}}$ is the composite energy price, $\theta_{i,a}^{\text{VA}}$ is the reference value-added share, and σ_a^{KLE} is the substitution elasticity between energy and value-added. The value-added cost $p_{i,a}^{\text{VA}}$ is a composite of plant-specific factor prices $\boldsymbol{\omega}_{i,a,f}$ (e.g., labor and capital). The energy and material prices, $p_{i,a}^{\text{Ene}}$ and $p_{i,a}^{\text{Mat}}$, are themselves CES composites that aggregate specific energy carriers $e \in \mathcal{E}$ and material inputs $m \in \mathcal{M}$:

$$p_{i,a}^{\text{Ene}} = \left[\sum_{e\in\mathcal{E}} \theta_{i,a,e}(p_{i,a,e})^{1-\sigma_a^{\text{Ene}}}\right]^{\frac{1}{1-\sigma_a^{\text{Ene}}}} \tag{4}$$

$$p_{i,a}^{\text{Mat}} = \left[\sum_{m\in\mathcal{M}} \theta_{i,a,m}(p_{i,a,m})^{1-\sigma_a^{\text{Mat}}}\right]^{\frac{1}{1-\sigma_a^{\text{Mat}}}} \tag{5}$$

where $\mathcal{E} = \{\text{coal, natural gas, electricity}\}$ and $\mathcal{M}$ includes primary iron units and scrap. [8]

[6] This behavioral assumption is supported by the low degree of global market concentration; the largest firm controls approximately 5% of output and the global Herfindahl-Hirschman Index (HHI) remains below 125. While domestic production is concentrated in some regions, the pricing of marginal units is disciplined by international trade exposure and the diverse cost structures of hundreds of individual production units. See Table C2 in the Appendix for detailed concentration metrics.

[7] Constant returns to scale at the plant level ensures that producer prices equal unit costs. While each unit has a flat marginal cost, the global supply curve remains upward-sloping due to plant-level cost heterogeneity and the implicit capacity limits imposed by sluggish factor mobility (eq. 6).

[8] We allow for idiosyncratic price dispersion at the plant level to reflect local market frictions. Regional aggregate supplies—whether primary endowments or Armington composites—are transformed into plant-specific inputs ($\omega_{i,a,f}$) via a constant elasticity of transformation (CET) frontier:

$$\omega_{i,a,f} = \Omega_{r,f}\left[\theta_{i,a,f}^{F}\left(\frac{q_{i,a,f}}{Q_{r,f}}\right)\right]^{\frac{1}{\eta_f^F}}, \tag{6}$$

The user cost of each energy carrier $p_{i,a,e}$ reflects the regional carbon price τ_r:

$$p_{i,a,e} = \omega_{i,a,e} + \tau_r \epsilon_{i,a,e}, \tag{8}$$

where $\omega_{i,a,e}$ is the plant-specific pre-tax cost of energy carrier e (governed by the mobility frontier defined in 6), τ_r is the regional carbon price, and $\epsilon_{i,a,e}$ is the carbon intensity per unit of energy (measured in tCO_2 per physical unit of energy carrier e). Note that we distinguish between the plant's emissions intensity per energy source, $\epsilon_{i,a,e}$, and its product-level intensity, $\epsilon_{i,a,v}$ (measured in tCO_2 per tonne of output), which accounts for the full metallurgical process including upstream iron production. That distinction is central because BCAs apply to embodied product emissions, not directly to individual energy inputs. The limited substitutability within these nests ($\sigma_a^{\text{KLE}}, \sigma_a^{\text{Ene}}$) formally represents the sector's hard-to-abate nature, as plants cannot easily switch away from carbon-intensive fuels in response to τ_r.

TRANSFORMATION INTO INTERMEDIATE AND FINAL VARIETIES.—Semi-finished products are transformed into variety-specific outputs $v \in \mathcal{V}$ according to a CET frontier. For ironmaking technologies $a \in \mathcal{A}_I$, this yields intermediate iron varieties ($v \in \mathcal{V}_I$), while steelmaking technologies $a \in \mathcal{A}_S$ produce finished steel varieties ($v \in \mathcal{V}_S$). The supply of a specific variety v from plant i is given by:

$$q_{i,a,v} = \theta_{i,a,v} Q_{i,a} \left(\frac{p_{i,a,v}}{c_{i,a}} \right)^{\tau_a} \tag{9}$$

where $q_{i,a,v}$ is the quantity of variety v produced, $Q_{i,a}$ is the total activity level of the plant, $p_{i,a,v}$ is the variety price, τ_a is the transformation elasticity, and $\theta_{i,a,v}$ is the reference volume share of variety v in technology a's output.

VERTICAL SUPPLY CHAINS AND IRON SOURCING.—A defining feature of the model is the vertical linkage between the iron and steel stages. Because carbon emissions are primarily concentrated in the ironmaking stage, steelmaking technologies ($a \in \mathcal{A}_S$) face a strategic supply chain choice: produce iron intermediate inputs $v \in \mathcal{V}_I$ internally (onsite integration) or purchase them from the regional merchant market. The effective user cost $p_{i,a,v}^{\text{Iron}}$ for a steelmaker is a CES composite:

$$p_{i,a,v}^{\text{Iron}} = \left[\theta_{i,a,v}^{\text{Iron}} (p_{i,a',v})^{1-\sigma_v^{\text{Iron}}} + (1 - \theta_{i,a,v}^{\text{Iron}}) (P_{r,v})^{1-\sigma_v^{\text{Iron}}} \right]^{\frac{1}{1-\sigma_v^{\text{Iron}}}} \tag{10}$$

where $p_{i,a',v}$ is the cost of iron produced onsite using technology $a' \in \mathcal{A}_I$, $P_{r,v}$ is the regional price of the Armington iron composite, $\theta_{i,a,v}^{\text{Iron}}$ is the plant-specific reference onsite share, and σ_v^{Iron} is the substitution elasticity between onsite and merchant iron.

This representation formally describes the carbon supply chain, explicitly capturing how upstream carbon costs are transmitted to downstream steel varieties and when underpriced imported intermediates can displace taxed domestic integrated iron.

where $q_{i,a,f}$ is the quantity of input f allocated to plant i and η_f^F is the transformation elasticity governing mobility. This captures the sluggishness in reallocating specialized resources, including localized constraints in logistics or contracting for energy and materials, between specific industrial sites.

Input demand can be derived by differentiating the unit cost function with respect to input prices according to Shephard's Lemma:

$$q_{i,a,f} = Q_{i,a} \frac{\partial c_{i,a}}{\partial \omega_{i,a,f}}, \tag{7}$$

where $Q_{i,a}$ is the total activity level of the plant. These substitution margins across the nested production structure ($\sigma_a, \sigma_a^{\text{KLE}}, \sigma_a^{\text{Ene}}, \sigma_a^{\text{Mat}}$) are the structural drivers of what the results later decompose as the "technique effect" (see Section V.C).

B. Linking Plants to Output and Input Markets

This block links the industrial layer to regional goods markets, downstream demand, and the broader system of goods and factor markets. It is therefore central for quantifying both the scale margin, through demand compression, and the composition margin, through substitution across origins and varieties.

TRADE IN STEEL AND RAW MATERIALS.—In each region r, the total supply of steel varieties and tradable raw materials (factors $f \in \mathcal{F}_{\text{tradable}}$) is formed by aggregating domestic and imported quantities through a nested CES (Armington) structure. For each commodity $j \in \mathcal{V} \cup \mathcal{F}_{\text{tradable}}$, the regional price index $P_{r,j}$ is:

$$P_{r,j} = \left[\theta^A_{r,j}(P^D_{r,j})^{1-\sigma^A_j} + (1-\theta^A_{r,j})(P^M_{r,j})^{1-\sigma^A_j}\right]^{\frac{1}{1-\sigma^A_j}}, \tag{11}$$

where $P^D_{r,j}$ and $P^M_{r,j}$ are the prices of the domestic and imported composites, respectively. The domestic composite price $P^D_{r,j}$ aggregates local supply from plants $i \in \mathcal{I}_r$ for steel, or local resource extraction for raw materials. The imported bundle price $P^M_{r,j}$ similarly aggregates bilateral imports across foreign origins $s \neq r$ using the substitution elasticity σ^M_j:

$$P^M_{r,j} = \left[\sum_{s\neq r} \theta^M_{s,r,j}(p_{s,r,j})^{1-\sigma^M_j}\right]^{\frac{1}{1-\sigma^M_j}}, \tag{12}$$

where $p_{s,r,j}$ is the price of commodity j exported from region s to region r, accounting for trade costs and applicable border taxes. This Armington structure ensures that the model captures the idiosyncratic trade patterns and cross-border price transmission for both industrial goods and upstream inputs, and governs how strongly border charges pass through into destination-market prices and trade shares.[9]

MACRO-PRODUCTION.—The aggregate macroeconomic sector (Mac) produces the intermediate macro-good $Q_{r,Mac}$ by bundling primary factors, macro-intermediates, and Armington steel varieties $v \in \mathcal{V}_S$. The unit cost $P_{r,Mac}$ is the dual of the nested CES production function:

$$P_{r,Mac} = \mathcal{C}_{r,Mac}(\Omega_{r,f}, P_{r,v}, \dots), \tag{14}$$

and the resulting demand for each steel variety v is $Q_{r,Mac,v} = Q_{r,Mac}(\partial P_{r,Mac}/\partial P_{r,v})$. Finally, the consumption bundle $Q_{r,C}$ is produced using the macro-good as the primary input, with its price $P_{r,C}$ serving as the numeraire or being endogenously determined. This block is what maps changes in steel prices into downstream user prices, aggregate demand, and ultimately welfare.

MARKETS FOR STEEL VARIETIES AND MATERIAL INPUTS.—For each steel variety and tradable raw material $j \in \mathcal{V} \cup \mathcal{F}_{\text{tradable}}$, the total quantity supplied by region r must equal the

[9] The demand for a specific plant-level variety of finished steel $q_{i,r,a,v}$ in destination region r is derived from the Armington composites via Shephard's Lemma. For a given total regional demand $Q_{r,v}$, the quantity sourced from plant i in region s is:

$$q_{i,r,a,v} = Q_{r,v}\frac{\partial P_{r,v}}{\partial p^x_{i,r,a,v}}. \tag{13}$$

sum of domestic demand and aggregate export demand:

$$Q_{r,j}^{\text{sup}} = q_{r,r,j}^{D} + \sum_{s \neq r} q_{r,s,j}^{M}, \tag{15}$$

where $Q_{r,j}^{\text{sup}}$ is the total regional production (summed across plants for steel, or local resource extraction for materials), $q_{r,r,j}^{D}$ is domestic demand, and $q_{r,s,j}^{M}$ denotes aggregate bilateral exports from region r to destination s. The global equilibrium requires that these bilateral exports strictly equal the sum of import demands from the destination region. For steel varieties v, this bilateral trade identity is:

$$q_{r,s,v}^{M} = \sum_{i \in \mathcal{I}_r} \sum_{a \in \mathcal{A}} q_{i,s,a,v}, \tag{16}$$

which formally maps the plant-to-region derived demand from (13) into the regional export flow.

MARKET FOR MACRO GOOD.—The regional market for the macroeconomic good Mac clears when the total output $Q_{r,Mac}$ equals the sum of intermediate demand from the steel sector and final consumption demand from the household:

$$Q_{r,Mac} = \sum_{i,a} q_{i,a,Mac} + Q_{r,Mac}^{C}, \tag{17}$$

where $Q_{r,Mac}^{C}$ is the quantity of the macro-good used to produce the final consumption bundle $Q_{r,C}$.

PRIMARY FACTOR MARKETS.—Each region r is endowed with a set of primary factors $f \in \mathcal{F}$, including labor, capital, and raw materials (e.g., iron ore, coking coal, and steel scrap). Labor and capital are supplied perfectly inelastically, while raw materials are supplied price-elastically (with elasticity η_f). The factor market for f is in equilibrium if supply supply $Q_{r,f}$ equals the aggregate demand from all production activities:

$$Q_{r,f} = \sum_{i,a} q_{i,a,f} + q_{r,Mac,f}, \tag{18}$$

where $q_{i,a,f}$ is the plant-level factor demand and $q_{r,Mac,f}$ is the demand from the macro-sector.

C. *Climate-Trade Policies*

This blocks describes how the climate-trade policy instruments are represented in the quantitative model. Domestic carbon pricing raises the cost of carbon-intensive production at source, while the BCA prices embodied emissions at the trade interface either on a mass basis or relative to a benchmark.

REGIONAL CARBON PRICING ON ENERGY.—A regional carbon price τ_r is levied on the carbon content of energy carriers $e \in \mathcal{E}$ used in production. As established in (2), this enters the producer's cost directly through the energy price $p_{i,a,e}$. Total regional emissions from the steel sector $Q_{r,CO2}$ are:

$$Q_{r,CO2} = \sum_{i \in \mathcal{I}_r} \sum_{a \in \mathcal{A}} \sum_{e \in \mathcal{E}} \epsilon_{i,a,e} q_{i,a,e}, \tag{19}$$

where $\epsilon_{i,a,e}$ is the carbon intensity per unit of energy carrier e.

BORDER CARBON ADJUSTMENTS ON EMBODIED CARBON.—While regional pricing applies

to inputs, BCAs are applied to the total carbon embodied in finished varieties v. The embodied emissions intensity $\epsilon_{i,a,v}$ accounts for direct process emissions and energy-related emissions across the metallurgical supply chain. Under a mass-based BCA, the destination region r levies a charge on imports from plant i in region s:

$$p^x_{i,r,a,v} = p_{i,a,v} + \tau_r \epsilon_{i,a,v}. \tag{20}$$

Under a rate-based BCA, the destination region sets an intensity target $\bar{\psi}_{r,v}$. Exporters must surrender permits covering their actual emissions $\epsilon_{i,a,v}$ while receiving credits based on the target $\bar{\psi}_{r,v}$. The export price is:

$$p^x_{i,r,a,v} = p_{i,a,v} + \nu_{r,v}(\epsilon_{i,a,v} - \bar{\psi}_{r,v}), \tag{21}$$

where $\nu_{r,v}$ is the shadow price of the intensity constraint. The value of $\nu_{r,v}$ is determined endogenously by the permit market-clearing condition. Relative to (20), the benchmark term introduces the credit that attenuates the effective border price in the rate-based design.[10] All policy-generated revenues, including carbon tax proceeds and border adjustment wedges, are redistributed to households in the same region.

D. *Aggregate Resource Constraints*

The model is closed by aggregate budget constraints of the continuum of representative households in each region. Households receive income I_r from factor returns, the benchmark trade imbalance $\bar{\Delta}_r$, and revenues from climate-trade policy:

$$I_r = \sum_{f \in \mathcal{F}} \omega_{r,f} E_{r,f} + \bar{\Delta}_r + TR_r, \tag{23}$$

where $E_{r,f}$ is the resource endowment and TR_r represents total transfers from carbon pricing and border adjustments. TR_r denotes total regional transfers defined as:

$$TR_r = \tau_r Q_{r,CO2} + \sum_{v \in \mathcal{V}} \sum_{s \neq r} \sum_{i \in \mathcal{I}_s} \sum_{a \in \mathcal{A}} (p^x_{i,r,a,v} - p_{i,a,v}) q_{i,r,a,v}, \tag{24}$$

where the first term represents domestic carbon pricing revenue and the second term represents the net proceeds (or "feebate" balance) from BCAs on all imported varieties.

Households spend this income on the aggregate final consumption bundle $Q_{r,C}$:

$$P_{r,C}\, Q_{r,C} = I_r, \tag{25}$$

where the consumer price index $P_{r,C}$ is endogenously determined by the underlying macro-production technology.

E. *Equilibrium*

For a given set of climate policy instruments—characterized by regional carbon prices τ_r, intensity targets $\bar{\psi}_{r,v}$, and permit-clearing rules—a competitive equilibrium is defined as a vector of prices $\mathcal{P} = \{p_{i,a,v}, P_{r,j}, \Omega_{r,f}, \omega_{r,f}, P_{r,Mac}, P_{r,C}, \nu_{r,v}\}$, quantities $\mathcal{Q} =$

[10] In regions implementing rate-based BCAs, the permit market clears when the net embodied emissions of imports satisfy the intensity target. The permit price $\nu_{r,v}$ is non-negative and is strictly positive only if the aggregate intensity of imports from all regions $s \neq r$ binds at the target $\bar{\psi}_{r,v}$:

$$\sum_{s \neq r} \sum_{i \in \mathcal{I}_s} \sum_{a \in \mathcal{A}} (\epsilon_{i,a,v} - \bar{\psi}_{r,v}) q_{i,r,a,v} \leq 0. \tag{22}$$

$\{q_{i,r,a,v}, Q_{r,j}, Q_{r,f}, Q_{r,Mac}, Q_{r,C}\}$, and regional incomes $\mathcal{I} = \{I_r\}$ such that consumers and firms optimize and all markets clear. Households maximize utility subject to the budget constraint (23), which determines demand for the final consumption bundle $Q_{r,C}$. Firms take prices as given and choose inputs and outputs to maximize profits, equivalently minimize costs under constant returns to scale. At the plant level, this yields unit costs $c_{i,a}$ and input demands governed by (2)–(7); at the aggregate level, the macro sector minimizes the cost of producing $Q_{r,Mac}$ according to (14). Under perfect competition, these firm optimization conditions imply zero profits and prices equal to corresponding unit costs, including variety prices $p_{i,a,v}$ and Armington price indices $P_{r,j}$. Market-clearing identities hold globally for steel varieties and material inputs (15), with bilateral trade satisfying (16), and regionally for the macro good (17) and factor markets (18). In regimes with rate-based BCAs, the permit price $\nu_{r,v}$ clears the intensity permit market according to (22).

IV. Data and Calibration

This section describes the empirical foundation of the quantitative model. We first summarize the data sources used to measure plant-level heterogeneity, trade linkages, and the broader macroeconomic environment. We then explain how these sources are combined to construct the baseline equilibrium that anchors the counterfactual analysis, and finally summarize the calibration of the structural parameters that govern behavioral responses.

A. Data Sources

The empirical foundation of the model combines plant-level industrial data, international trade statistics, and national accounts.

INDUSTRIAL MICRO-DATA.—Data for the industrial layer are drawn primarily from the CRU Steel Cost Service, which reports production volumes, technology portfolios, unit costs, and detailed energy and material input coefficients for roughly 300 steel mills across 48 countries. We use the Global Steel Plant Tracker (GSPT) to assess the capacity coverage of the CRU sample. As shown in Panel (a) of Table 1, the cleaned sample demonstrates the global representativeness of the dataset, capturing 55.9% of world production, 70.3% outside China, and 98.0% of the integrated BF-BOF fleet outside China (CRU Group, 2023; Global Energy Monitor, 2023). Ultimately, plant-level output is reweighted to match regional production aggregates from the World Steel Association (worldsteel) Statistical Yearbooks, and its implied trade linkages are reconciled with observed bilateral customs data, ensuring that our granular baseline is consistent with global commodity flows (World Steel Association, 2022).

TRADE AND MARGINS.—Bilateral trade flows for finished steel and merchant iron are sourced from UN Comtrade at the HS 6-digit level. Trade in primary raw materials is assembled from UN Comtrade for iron ore and scrap, the U.S. Energy Information Administration (EIA) for metallurgical coal, and the BP Statistical Review for natural gas. To discipline exporter participation and trade margins, we use OECD sources on firm counts, exporting behavior, and international transport costs (United Nations Statistics Division, 2024; U.S. Energy Information Administration, 2024; BP, 2022; OECD, 2021, 2024*b*,*c*,*a*).

MACROECONOMIC FRAMEWORK.—The broader macroeconomic environment is anchored to GTAP 11 (Aguiar et al., 2022), which provides the national accounts and trade structure used to embed the steel sector in general equilibrium.[11]

[11]The model distinguishes 15 regions: EU-28 and European Free Trade Association (EUR), United States (USA), China (CHN), India (IND), Japan (JPN), South Korea (KOR), Other Asia (OAS), Oceania (OCE), Canada (CAN), Mexico (MEX), Brazil (BRA), Other South America (OSA), Turkey and Other Europe (OEU), CIS and Ukraine (CIS), and Western Asia and Africa (WAF).

B. *Constructing the Baseline Equilibrium*

We combine these sources to construct the baseline equilibrium. Throughout the remainder of this section, reference data objects corresponding to endogenous model variables are denoted with an overbar. The baseline allocation is therefore summarized by $\{\overline{Q}_{i,a}, \overline{q}_{i,a,f}, \overline{q}_{i,s,a,v}, \overline{\epsilon}_{i,a,v}\}$, where the overbar indicates the factual reference equilibrium. The construction proceeds in four steps.

SAMPLE SELECTION AND VALIDATION.—We begin by cleaning the raw plant records, dropping facilities with incomplete or inconsistent operational accounts, and mapping plant locations into the model's regional aggregation. This step is needed to preserve the plant-level heterogeneity that is central to the analysis while ensuring that the sample remains representative at the regional and technological level. We assess the resulting coverage against GSPT and worldsteel references and use these external controls to verify that the final sample captures the observed global distribution of capacity and production. Appendix B.B1 reports the full sample-selection, cleaning, and region-mapping procedure.

PROCESS MODELING AND CARBON ACCOUNTING.—The engineering accounts reported by CRU do not map one-for-one into the model's production structure. We therefore aggregate detailed subprocesses into the model's ironmaking and steelmaking technologies, trace how upstream activities such as raw material preparation feed into the relevant production routes, and separate captive from merchant iron flows. We also reverse the conventional accounting treatment of process gases and other byproducts as revenue credits, so that carbon accounting follows gross physical energy use rather than net financial cost. This step is essential for measuring embodied emissions consistently across integrated and merchant supply chains. Appendix B.B2 provides the full process-modeling and carbon-accounting procedure.

REGIONAL BALANCES.—Next, we reconcile the bottom-up plant data with top-down production and material balances. Plant-level output is reweighted to match worldsteel totals by region and product while preserving within-region heterogeneity. For iron ore, scrap, natural gas, and metallurgical coal, we combine bottom-up input requirements with production and trade statistics to construct physically consistent regional balances. The purpose is to anchor the baseline in observed production scales and resource constraints before introducing any counterfactual policy wedges. Appendix B.B3 details the balancing procedure.

TRADE FLOW IMPUTATION.—Finally, aggregate customs data must be translated into plant-level trade linkages. We estimate a gravity equation using OECD data to discipline the extensive margin of exporting across region pairs, then assign export participation across plants using a Ricardian ranking by unit costs. By Ricardian ranking, we mean that lower-cost plants are more likely to serve foreign markets and are therefore selected into exporting first. We then reconcile plant-destination flows to observed bilateral trade matrices. This step matters because the policy experiments work through the reallocation of sales across plants, destinations, and positions in the supply chain. Appendix B.B4 reports the full trade-imputation procedure.

C. *Calibration Strategy and Parameters*

Table 1 provides the empirical foundation for our calibration, summarizing the key characteristics of our plant-level sample and the input shares that govern behavioral responses.

CALIBRATION STRATEGY.—We calibrate the model using the calibrated-share-form approach standard in multisector general equilibrium analysis (Rutherford, 1995; Hertel, 1997; van der Mensbrugghe, 2019). The data-construction step delivers the baseline objects $\{\overline{Q}_{i,a}, \overline{q}_{i,a,f}, \overline{q}_{i,s,a,v}, \overline{\epsilon}_{i,a,v}\}$, which we treat as the reference equilibrium. Plant-level output and engineering accounts pin down baseline activity levels and nested input shares,

Table 1. Descriptive Statistics and Empirical Input Shares

Panel A: Sample Characteristics and Overview

			Plant-level Measure		
	Plants (N)	**Total Prod. (Mt)**	**Prod. (Mt)**	**Unit Cost (USD/t)**	**CO_2 Int. (tCO_2/t)**
Steelmaking	284	1049.46	3.37	434.40	1.53
		(55.9%)	(3.54)	(51.58)	(1.09)
By Technology Route:					
Integrated (BOF)	162	852.22	5.26	449.61	2.36
		(63.3%)	(3.91)	(53.03)	(0.54)
Secondary (EAF)	149	197.24	1.32	417.87	0.62
		(37.8%)	(1.26)	(44.55)	(0.77)
By Region:					
China	66	430.04	5.51	449.96	2.14
		(43.2%)	(4.42)	(29.13)	(0.79)
Rest of World	218	619.42	2.66	429.20	1.33
		(70.3%)	(2.87)	(56.25)	(1.10)
By Product Category:					
Flat Steel	161	670.32	4.16	437.26	1.98
		(83.0%)	(3.51)	(53.77)	(0.89)
Long Steel	200	379.14	1.90	431.93	1.38
		(42.7%)	(1.79)	(49.52)	(1.11)
Ironmaking	189	886.23	4.45	346.31	2.32
		(62.8%)	(3.64)	(62.63)	(0.70)
By Technology Route:					
Blast Furnace (BF)	164	820.10	5.00	362.71	2.55
		(63.1%)	(3.72)	(46.11)	(0.35)
Direct Reduction (DR)	35	66.14	1.89	269.43	1.24
		(59.2%)	(1.60)	(72.58)	(0.91)

Panel B: Comparison of Production Routes

	Ironmaking		**Steelmaking**	
Empirical Measure (%)	**BF**	**DRF**	**BOF**	**EAF**
Material Share of Total Cost	45.0 (7.8)	61.7 (19.6)	83.6 (5.0)	71.1 (5.9)
Energy Share of KLE Cost	78.0 (5.5)	66.3 (16.3)	9.3 (3.5)	35.9 (9.2)
Labor Share of Value-Added	30.4 (13.0)	27.4 (18.6)	26.8 (14.1)	17.3 (10.5)
Elec. Share of Energy Cost	7.4 (2.6)	19.7 (10.7)	90.7 (10.9)	91.7 (4.8)
Coal Share of Energy Cost	88.7 (7.2)	22.8 (33.8)	1.7 (2.9)	4.6 (3.5)
Gas Share of Energy Cost	3.9 (7.5)	57.5 (34.9)	7.7 (10.9)	3.7 (2.7)
Quantity Share of Scrap	1.2 (1.6)	0.4 (2.3)	11.7 (6.6)	73.4 (31.9)
Captive Iron Share	–	–	96.2 (17.4)	21.5 (37.6)
Specialized Plants (>95% single product)	–	–	61.7	80.5

Notes: Panel (a) reports sample counts and production-weighted means (standard deviations in parentheses) for plants in the cleaned sample. Production coverage is relative to worldsteel 2019 reference values. Panel (b) reports production-weighted mean shares (%). Figures in parentheses are standard deviations across plants. Captive iron share is the percentage of iron units sourced from onsite ironmaking technology. Specialized plants are defined as those where flat or long products account for more than 95% of total output. Source: Own calculations based on CRU Group (2023) and World Steel Association (2022)

while the imputed plant-destination flows pin down the baseline transformation, sourcing, and trade shares needed to reproduce the observed allocation. Conditional on reference prices and policy wedges, the share parameters of the model are chosen so that the numerical equilibrium exactly replicates these baseline objects.[12] The model solves for the profit-maximizing output, sourcing, and trade decisions of each of the 284 individual plants

[12]This differs from the structural inversion exercises common in modern quantitative trade models, where latent productivity or trade-cost objects are recovered from a parsimonious equilibrium system; see, for example, Eaton and Kortum (2002), Anderson and van Wincoop (2003), and Costinot and Rodríguez-Clare (2014). Here a rich baseline allocation is observed directly, and calibration maps those data into a share system that reproduces the baseline exactly.

independently.

FREE PARAMETERS.—Conditional on these reference shares, the remaining free parameters govern substitution across trade origins, input adjustment within plants, and vertical sourcing between integrated and merchant iron. Table C1 summarizes the full parameterization. Because exact econometric estimates for highly granular intra-plant substitution are scarce, we combine macroeconomic trade parameters, such as the Armington elasticities (σ^A, σ^M) and the consumption substitution elasticity (σ^C), drawn from the GTAP database, with calibrations grounded in the metallurgical realities shown in Panel (b) of Table 1. For the plant-level nests, elasticities ($\sigma_a, \sigma_a^{\text{KLE}}, \sigma_a^{\text{VA}}, \sigma_a^{\text{Ene}}$) are set low to reflect stoichiometric and thermal rigidities. For instance, the tightly clustered BOF scrap shares (11.7% mean, 6.6% SD) are consistent with an inelastic material substitution elasticity ($\sigma_{\text{BOF}}^{\text{Mat}} = 0.3$), while the high variance in EAF scrap shares (73.4% mean, 31.9% SD) allows for greater flexibility ($\sigma_{\text{EAF}}^{\text{Mat}} = 2.5$). Similarly, the near-universal reliance on captive iron in BOF plants (96.2% mean, 17.4% SD) is reflected in an inelastic sourcing elasticity ($\sigma_v^{\text{Iron}} = 0.1$) to account for the thermal and logistical penalties of unbundling integrated sites.

Beyond the core production nests, the model calibrates several parameters governing supply-side and demand-side heterogeneity. The transformation elasticity (τ_a) governs the supply-side capability to shift from semi-finished steel into specific product varieties (flat vs. long). A substantial majority of plants are highly specialized, with 61.7% of BOF plants and 80.5% of EAF plants producing almost exclusively ($> 95\%$) a single product category. This physical lock-in to installed rolling capital justifies our calibration of τ_a as rather inelastic. On the demand side, the within-domestic variety substitution (σ_v^D) captures how downstream users switch between domestic plants. Finally, factor market rigidities are captured by the price elasticity of factor supply (η_f), distinguishing between the relatively inelastic structural constraints of circular scrap recovery and the highly elastic supply of primary resources, as well as transformation elasticities restricting plant-level mobility of capital and labor (η_f^F). These parameter choices determine how strongly nominal policy wedges are transmitted into changes in production, trade, vertical sourcing, and welfare. To ensure our core findings are not artifacts of these point estimates, we subject the most critical structural and behavioral parameters to an extensive sensitivity analysis in Section V.E.

V. Counterfactual Policies: Model-Based Estimates

This section uses the calibrated model to quantify how BCA architecture shapes the trade-off between environmental ambition and economic protection. The results speak directly to the paper's central design question: how much climate ambition is transmitted abroad, through which margins adjustment occurs, and how protection is allocated across the supply chain.

We proceed in four steps. First, we compare mass-based and rate-based BCAs in the symmetric EU paradigm and the asymmetric US paradigm to quantify cost-effectiveness at common stringency and, using discounted mass-based comparisons, at common global emissions outcomes. Second, we trace the mechanisms behind that ranking by decomposing adjustment into scale, composition, technique, reshuffling, and vertical-leakage margins. Third, we examine incidence across regions and between upstream producers and downstream users. Finally, we show that the ranking and the main mechanisms are robust to alternative parameter values.

A. Design of Counterfactual Experiments

We evaluate the structural properties of border carbon adjustments through a series of counterfactual experiments. These experiments are designed to separate the effects of

instrument architecture from the effects of overall policy stringency and from the presence or absence of a domestic carbon-price anchor.

POLICY PARADIGMS.—We study two paradigms. In the *symmetric paradigm*, the BCA complements an existing domestic carbon price, as in the EU. In the *asymmetric paradigm*, the BCA operates as a standalone instrument in a region without a domestic price, as in the US. In addition to the *Global Cap* first-best benchmark and the unilateral *EU Cap*, we compare mass-based and rate-based border instruments in each paradigm. The *EU M-BCA* extends τ_{EUR} to the full embodied emissions of imports, while the *EU R-BCA* replaces that tariff with a benchmarked rate-based standard. The benchmark $\bar{\psi}_{r,v}$ is set to the emissions intensities of imports in the corresponding mass-based case so that the comparison focuses on architecture rather than baseline calibration. In the US, the *US M-BCA* and *US R-BCA* provide the analogous standalone comparison at a border price equal to the EU ETS price.

We select a 30% reduction in EU domestic steel emissions as our primary point of comparison. This stringency level is aligned with the European steel industry's decarbonization pathway under the Fit for 55 package, which aims for a 55% reduction by 2030 relative to 1990 levels—approximately 30% below our 2019 baseline (European Steel Association, 2020).

ACCOUNTING SCOPE AND FACILITY BOUNDARIES.—We measure embodied emissions comprehensively, including direct process emissions, indirect electricity emissions, and emissions from upstream intermediates such as ironmaking. This broader boundary is useful for evaluating long-run BCA design, even though current implementations such as the EU CBAM initially apply narrower coverage. Facility boundaries matter because both rate-based and mass-based designs assess liability using the exporting plant's declared intensity. By modeling trade in both finished steel ($v \in \mathcal{V}_S$) and intermediate iron ($v \in \mathcal{V}_I$), we can therefore quantify whether incomplete tracking of upstream emissions creates vertical leakage, as in Section II.

DISCOUNTED PRICE APPROACH.— Because equal domestic stringency does not imply equal global abatement, we also use the discounted-price comparison motivated by Proposition 1. For each rate-based policy, we solve for $\lambda \in [0, 1]$ such that a mass-based BCA with price $\lambda\tau_r$ delivers the same global emissions reduction. This environmentally equivalent benchmark lets us compare welfare and incidence holding global abatement constant, and λ directly measures the efficiency discount from signal dilution. This defines our discounted mass-based (DM-BCA) scenarios.

SCENARIO COMPARISON POINTS.—Throughout the results, we use a consistent set of comparison points to map these policies. Point A represents the unilateral EU Cap scenario with a 30% domestic emissions reduction target. Point B is the EU M-BCA scenario, where both domestic producers and importers face the same carbon price (approximately \$87.90/tCO_2) to achieve that 30% domestic reduction. To isolate the effect of policy architecture, the remaining points hold specific outcomes constant. In Point C (EU R-BCA), we hold import emissions intensity constant relative to the M-BCA by setting the rate-based benchmark exactly to the import emissions intensities that resulted from the M-BCA scenario in Point B. In Point D (EU DM-BCA), we hold global emissions reduction constant relative to the R-BCA. EU domestic producers face the full carbon price, but importers face a discounted BCA rate (λ) calibrated to achieve the exact same global emissions outcome as Point C.

In the asymmetric US paradigm, only importers face the carbon fee. Point E is the US M-BCA scenario, applying the same \$87.90/tCO_2 fee to imports. Following the same logic as the EU scenarios, Point F (US R-BCA) uses the benchmark import emissions intensities derived from the US M-BCA outcome, and Point G (US DM-BCA) applies a discounted tariff to match the global emissions reduction achieved under the US R-BCA

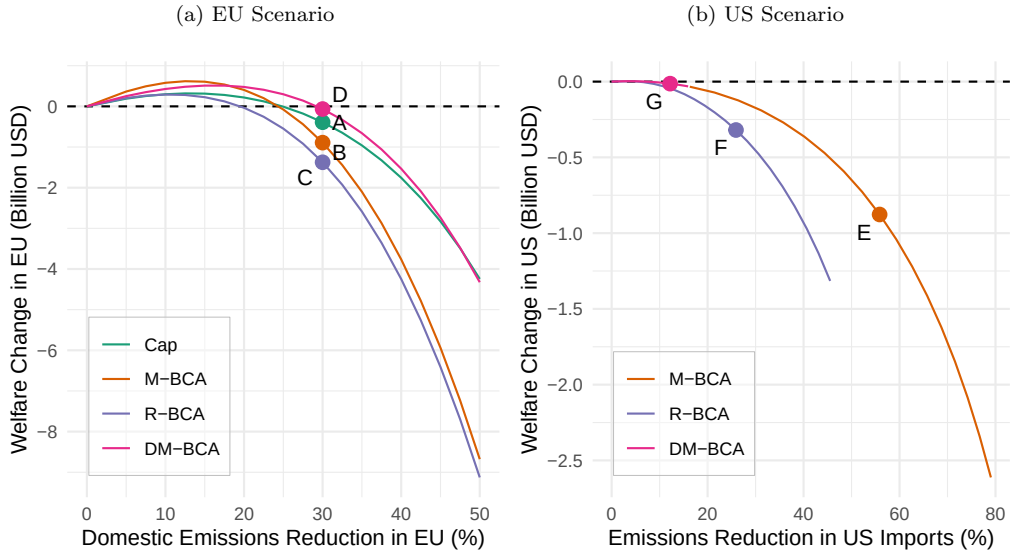

Figure 4. National Welfare Changes

Notes: Panel (a) plots EU welfare change (billion USD) against domestic emissions reduction in the EU (%). Panel (b) plots US welfare change (billion USD) against emissions reduction in US imports (%). Lines trace policy designs across stringency, and labeled points (A–G) mark the comparison points used in the analysis.

scenario.

B. Cost-Effectiveness and Carbon Signal Transmission

We begin with the aggregate ranking of policy designs. The key question is whether a rate-based BCA buys downstream relief at lower or higher cost once environmental ambition is held fixed, and how that answer depends on the presence of a domestic carbon-price anchor. Across both paradigms, the mass-based design delivers a stronger emissions signal and more abatement, whereas the rate-based design softens some price effects but does so by diluting the carbon signal transmitted abroad.

Figure 4 first shows how the two designs map domestic ambition into national welfare. We measure welfare as regional equivalent variation, so the figure reports the net economic burden of each policy relative to the baseline. In the EU case (Panel a), welfare initially rises at low stringency because terms-of-trade gains dominate domestic deadweight losses, but this advantage disappears as ambition increases. At the comparison point, the rate-based design (Point C) raises welfare losses by about 55% relative to the mass-based alternative ($1.38 billion versus $0.89 billion). Point D, the discounted mass-based BCA, achieves the same global emissions reduction as the rate-based design at a much lower cost (−$0.07 billion). Solving for environmental equivalence yields an implicit discount factor of $\lambda \approx 0.36$. In the language of Section II, the rate-based design therefore transmits only about 36% of the border price that the mass-based design requires to deliver the same global emissions outcome.

In the US case (Panel b), where there is no domestic carbon price to anchor the policy, the trade-off shifts. As shown in Table 2, the mass-based BCA (Point E) provides stronger industrial protection, increasing long-steel output by 1.11%, but it also imposes the higher welfare cost because consumers face larger price increases. The rate-based design (Point F) cuts that welfare cost by roughly two-thirds relative to the mass-based alternative (−$0.32 billion versus −$0.88 billion), but it also delivers only about one-quarter as much global abatement (0.06% versus 0.26%). As shown by Point G, the implicit discount factor falls to $\lambda \approx 0.12$. In the asymmetric paradigm, the rate-based border measure therefore

Table 2. Summary of Policy Impacts at Comparable Stringency Levels

Scenario	Global Emissions (%)	(Reverse) Leakage (%)	Domestic Welfare ($bn)	Domestic Output (%) Flat	Long	Macro	Carbon Price ($/tCO$_2$)
Panel (a): EU Scenarios							
A. Cap	−0.69	56.44	−0.39	−17.65	−6.68	−0.062	69.71
B. M-BCA	−1.34	16.05	−0.89	−16.25	−4.60	−0.126	87.90
C. R-BCA	−1.02	36.18	−1.38	−17.02	−6.19	−0.081	74.94
D. DM-BCA	−1.02	36.18	−0.07	−17.12	−5.79	−0.087	76.91
Panel (b): US Scenarios							
E. M-BCA	−0.26	(23.05)	−0.88	1.21	1.11	−0.018	87.90
F. R-BCA	−0.06	(14.93)	−0.32	0.40	0.86	−0.004	
G. DM-BCA	−0.06	(15.72)	−0.01	0.11	0.19	−0.003	10.19

Notes: Scenarios correspond to the points in Figure 4. Panel (a) presents EU policy options, all of which include the domestic ETS cap. Panel (b) presents US policy options, which are standalone border measures without a domestic price anchor. Scenarios are compared at a stringency level corresponding to a carbon price of approximately $88/tCO$_2$ (equivalent to a 30% domestic emissions reduction for the EU). Leakage rates in Panel (b) represent reverse leakage (onshoring).

transmits only about one-eighth of the nominal carbon price to foreign producers and provides little leverage for technology switching or fuel substitution abroad.

Figure 5 shows the same ranking from the global perspective. At the comparison point, the EU mass-based BCA (Point B) delivers about 31% more global emissions reduction than the rate-based design (1.34% versus 1.02%) at a lower welfare cost. By contrast, the US scenarios (Points E, F, G) exhibit a nearly vertical cost curve. Even with a mass-based tariff (Point E), the US policy achieves only limited global abatement (0.26%), and shifting to a rate-based design (Point F) cuts that already small effect by roughly three-quarters (0.06%). Part of this reflects the smaller volume of US imports, but the broader lesson is more general: without a domestic carbon-price anchor, border measures alone provide limited leverage for global decarbonization.

These patterns are the quantitative counterpart to Proposition 1. The implicit subsidy embedded in the rate-based design weakens the scale margin as a channel of abatement and forces adjustment toward costlier margins. That mechanism explains why the EU R-BCA (Point C) achieves less global abatement at higher welfare cost than the corresponding discounted mass-based design (Point D), and why the asymmetric paradigm produces such a steep cost curve once the border measure must operate without a domestic price anchor. This subsection therefore establishes the paper's baseline ranking: rate-based BCAs are a costlier way to deliver a given environmental outcome, and the loss is especially pronounced when the domestic carbon-price anchor is absent.

C. Abatement Margins, Reshuffling, and Vertical Leakage

The efficiency ranking is informative only if we also understand how the two instruments reallocate adjustment. We therefore turn to the mechanisms behind the results in Section V.B. The theory emphasized three channels in particular: dilution of the scale effect, reshuffling in heterogeneous downstream products, and vertical leakage in homogeneous upstream intermediates. The quantitative model allows us to measure the importance of each channel. The composition effect captures shifts across production routes, such as movement from integrated BF-BOF toward cleaner EAF production, while the technique effect captures within-plant efficiency changes such as fuel switching or energy-saving adjustments. These changes are structurally governed by the substitution elasticities defined in the plant-level nested production structure ($\sigma_a^{\text{Ene}}, \sigma_a^{\text{Mat}}, \sigma_a^{\text{KLE}}$) described in Section III.A.

VERTICAL LEAKAGE THROUGH MERCHANT IRON.—Panel (a) of Table 3 isolates where foreign emissions rise under the two EU policy designs. The rate-based design more than

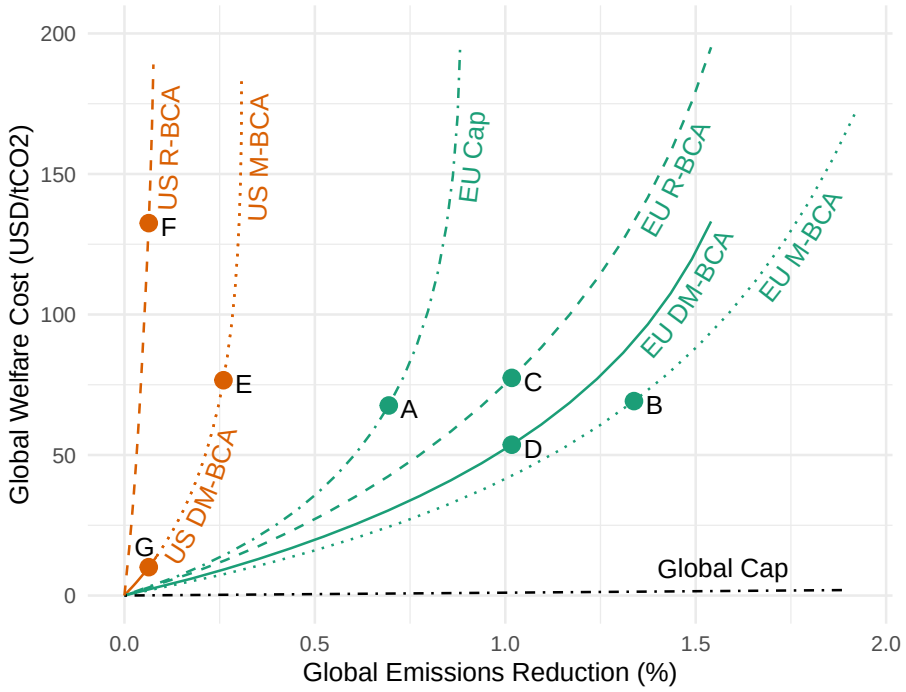

Figure 5. Global Cost-Effectiveness Frontier

Notes: Global emissions reduction (%) is plotted against global welfare cost (USD/tCO_2). Points trace policy designs across stringency in the EU and US scenarios.

Table 3. Mechanism Analysis of Emissions Changes in ROW

Panel (a): Sources of Emissions Change

Scenario	Steelmaking (i)	Ironmaking (ii) On-site	(iii) Merchant	Total
A. Cap	1.46	30.73	2.91	35.11
B. M-BCA	1.29	8.74	-0.04	9.98
C. R-BCA	2.57	14.57	5.36	22.50
D. DM-BCA	1.24	20.04	1.22	22.50

Panel (b): Decomposition of Steel and On-site Ironmaking Emissions (i + ii)

Scenario	Scale	Technique	Composition	Total
A. Cap	26.98	2.17	3.05	32.20
B. M-BCA	8.80	3.29	-2.06	10.03
C. R-BCA	17.24	2.88	-2.97	17.14
D. DM-BCA	17.29	2.66	1.34	21.28

Notes: Values represent CO_2 emissions changes in the Rest of the World (ROW) relative to the baseline in million tonnes (Mt). All scenarios are EU policy options, with the domestic ETS cap in place and at a stringency level corresponding to a 30% emissions reduction target. Panel (a) distinguishes between direct steelmaking (i), on-site ironmaking (ii), and merchant ironmaking (iii). Panel (b) decomposes the combined integrated emissions (i + ii) into scale, technique, and composition effects.

doubles the increase in Rest-of-World emissions relative to the mass-based alternative (22.50 versus 9.98 Mt CO_2). A central driver is the relocation of upstream iron production across borders. Under the EU R-BCA scenario, emissions from merchant ironmaking (Column 4) rise sharply, whereas they remain essentially flat under the mass-based scenario (5.36 versus −0.04 Mt).

This pattern is driven by the technological homogeneity of ironmaking, which triggers

the knife-edge sensitivity formalized in Section II. As shown in Table C3, the standard deviation of emissions intensity for pig iron imports is low (0.37) compared to long steel (1.01), reflecting chemical constraints of the BF that limit abatement even at high carbon prices. In our rate-based scenario, benchmarks are set to the emissions intensities of imports observed under the symmetric mass-based design. Because the intensity of pig iron remains rigid under these constraints, the calibrated benchmark (ψ) converges toward the actual intensity of all producers. As predicted by Lemma 3, this homogeneity renders the credit price highly sensitive to the benchmark level. In our simulation, the calibration lands on the zero-signal side of the knife-edge, effectively disabling the carbon price at the border. Table C3 confirms this asymmetry: the import price of pig iron remains about 41% lower under the rate-based design than under the mass-based alternative ($320/t versus $540/t). This price wedge induces the vertical leakage predicted by Proposition 7, allowing import volumes to more than double from 1.73 Mt under M-BCA to 3.50 Mt under R-BCA as downstream steelmakers substitute domestic integrated iron with under-taxed imports.

These magnitudes should not be read as frictionless short-run substitution. Integrated BOF plants are optimized for molten-iron charging, cold merchant pig iron entails a substantial thermal penalty, and the global merchant pig iron market remains small relative to total iron production. But these constraints do not undo the mechanism. They imply instead that vertical leakage is most likely to emerge through longer-run fleet reconfiguration, especially through EAF expansion using under-taxed imported pig iron as a high-purity feedstock. The broader lesson is that benchmarking a rigid upstream stage can unintentionally subsidize the offshoring of carbon-intensive intermediates.

SCALE, COMPOSITION, AND TECHNIQUE.—To characterize the remaining emissions response within steel production, we use the Logarithmic Mean Divisia Index (LMDI) decomposition. Following the identity $E = \sum_a (Y \cdot s_a \cdot e_a)$, where Y is total production, $s_a = Y_a/Y$ is the production share of technology a, and $e_a = E_a/Y_a$ is emissions intensity, we isolate three effects:

$$\Delta E = \underbrace{\sum_a w_a \ln\left(\frac{Y^1}{Y^0}\right)}_{\text{Scale Effect}} + \underbrace{\sum_a w_a \ln\left(\frac{s_a^1}{s_a^0}\right)}_{\text{Composition Effect}} + \underbrace{\sum_a w_a \ln\left(\frac{e_a^1}{e_a^0}\right)}_{\text{Technique Effect}} \tag{26}$$

where $w_a = \frac{E_a^1 - E_a^0}{\ln E_a^1 - \ln E_a^0}$ is the logarithmic mean weight, and superscripts 0 and 1 denote the baseline and policy scenario, respectively.

Panel (b) of Table 3 shows that the rate-based design (Row 3) induces a stronger negative composition effect, about 44% larger than under the mass-based design (-2.97 versus -2.06 Mt), indicating a larger shift toward cleaner production methods such as EAF for exports. This larger composition response is the aggregate manifestation of reshuffling toward cleaner export supply. But the gain is more than offset by the scale effect. Because rate-based measures lower the effective border price relative to full tariffs, they do not suppress global demand as much. The scale effect under EU R-BCA contributes to an emissions increase of 17.24 Mt, almost double the 8.80 Mt observed under the mass-based design. This is the composition–scale substitution in Proposition 2: once the scale margin is muted, the foreign sector relies more heavily on composition responses to satisfy the global emissions budget.

The technique effect, which reflects within-plant changes such as shifts in fuel mix or energy intensity, is essentially unchanged across designs, contributing around 3.0 Mt to the emissions increase. While this margin is similar in absolute magnitude to the structural shifts in technology mix, its stability across designs suggests that border measures primarily influence the high-level technological configuration of the industry (scale and

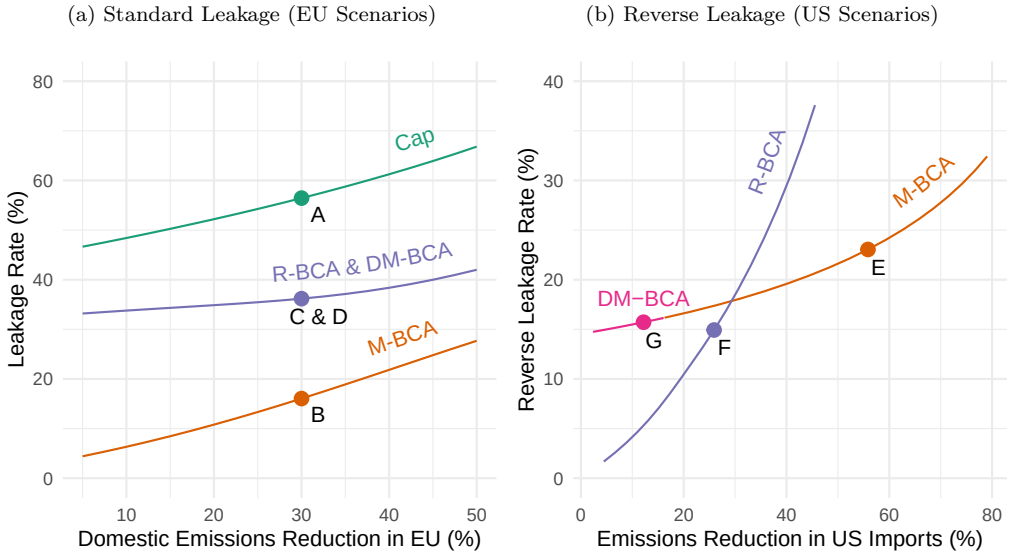

Figure 6. Leakage Dynamics

Notes: Panel (a) plots the leakage rate (%) against domestic emissions reduction in the EU (%) for EU policy scenarios. Panel (b) plots the reverse leakage rate (%) against emissions reduction in US imports (%) for US policy scenarios. Lines trace policy designs across stringency, and markers indicate the reference stringency used for comparisons.

composition) rather than the incremental efficiency of existing units.

REVERSE LEAKAGE IN THE ASYMMETRIC CASE.—The US case provides the mirror image. Figure 6 contrasts standard leakage in the EU (Panel a) with reverse leakage in the US (Panel b). Consistent with Brunel and Levinson (2024), the US tariff-only approach induces onshoring of pollution. By protecting domestic producers without a corresponding domestic carbon cost, the policy increases domestic production and offsets part of the decline in imports. This is the substitution effect in Proposition 6: without a domestic price anchor, the border measure behaves like an industrial tariff that reallocates production toward unabated domestic varieties rather than delivering much abatement abroad.

D. Incidence Across Regions and the Supply Chain

We next turn from environmental performance to incidence. The same benchmark subsidy that dilutes the emissions signal also reallocates rents across regions and between upstream producers and downstream users. In the EU case, rate-based designs raise national welfare losses by about 55% relative to the mass-based alternative (−$1.38 billion versus −$0.89 billion) because they do not price the full carbon content of imports. As Proposition 4 implies, the benchmark subsidy gives up fiscal revenue and the associated terms-of-trade gains.

REGIONAL INCIDENCE.—Figure 7 shows how this burden is redistributed across trading partners. Relative to the mass-based alternative, the EU's rate-based design increases the EU's own welfare loss while reducing losses for the US and the CIS region. Japan and Korea gain in both scenarios, and Other Asia (OAS) gains about eight times more under the rate-based design ($0.16 billion versus $0.02 billion under mass-based). The underlying reason is the same intensity benchmark: by penalizing the highest-intensity producers (China and India) most, it shifts relative advantage toward mid-intensity producers such as the CIS region and toward cleaner exporters such as Korea and OAS.

EXPORTER GAINS THROUGH RESHUFFLING AND VERTICAL LEAKAGE.—Trade volume analysis confirms this mechanism (Figure C2). Under the rate-based design, CIS pig iron

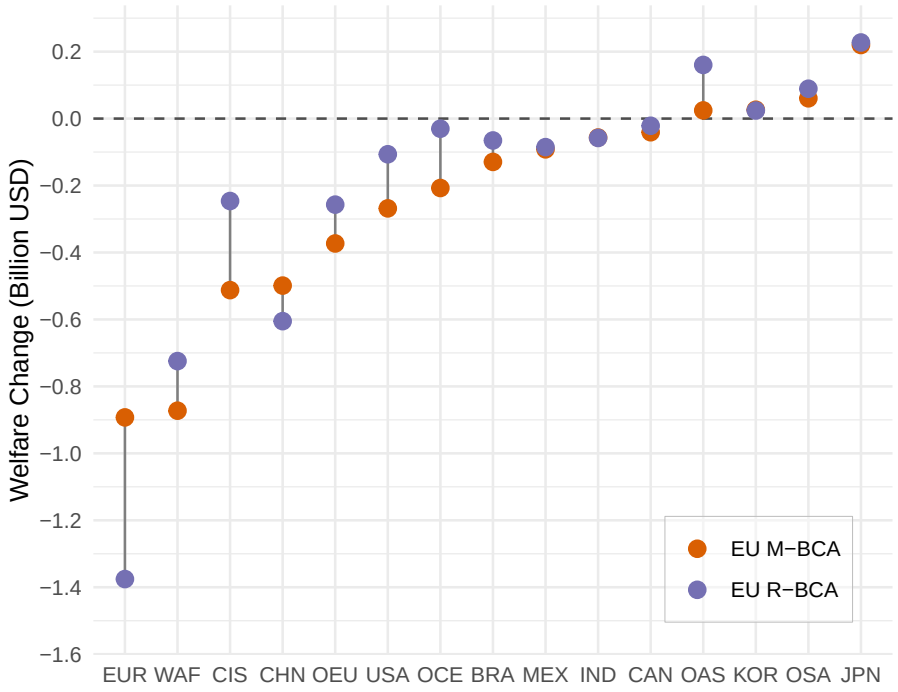

Figure 7. Regional Burden Sharing

Notes: Bars report regional welfare changes (billion USD) under the EU policy scenarios. Region codes: EU28/EFTA (EUR), US (USA), China (CHN), India (IND), Japan (JPN), South Korea (KOR), Other Asia (OAS), Oceania (OCE), Canada (CAN), Mexico (MEX), Brazil (BRA), Other South America (OSA), Turkey and Other Europe (OEU), CIS and Ukraine (CIS), and Western Asia and Africa (WAF).

exports rebound to 2.31 Mt, more than double the suppressed level under the mass-based design (1.03 Mt). The distributional gains for some upstream exporters therefore reflect the same vertical-leakage channel identified in Section V.C.

The surge in exports from regions like Japan and Korea is driven by resource reshuffling, a dynamic formalized in Section II. We define the Reshuffling Index (R) as the ratio of the emissions intensity of exports to the EU relative to the producer's domestic average intensity ($R = e_{exp}/e_{dom}$). As shown in Table C4, this strategic selection is restricted to sectors with high technological variance. The aggregate Reshuffling Index for the long steel sector falls from 1.08 to 0.55 under both border adjustment designs, while remaining nearly stagnant for the homogeneous pig iron sector (0.96). This disparity demonstrates that firms exploit technological heterogeneity to satisfy border standards without necessarily improving global production methods. At the regional level, this distortion is most pronounced for mixed-technology producers like Japan, where the index for long steel reaches 0.20, effectively diverting the clean capacity of the domestic market to satisfy the regulated market. This behavior empirically validates Proposition 3: at lower trade volumes, producers prioritize clean units to minimize taxes (Lemma 2), but as the rate-based design sustains higher volumes, this existing capacity is diluted, eventually forcing investment in new capacity to meet the standard.

DOWNSTREAM RELIEF AND UPSTREAM EXPOSURE.—Domestically, the main political attraction of the rate-based design is downstream price protection. Table 4 shows that at 30% stringency, the increase in user prices for flat steel is about 30% smaller under the rate-based design than under the mass-based alternative (24.2% versus 34.6%). This price differential reflects the effective border tax rate of $\lambda \approx 0.36$ identified in Section V.B: the rate-based design passes through only a fraction of the full carbon cost. The lower input cost is visible in macro outcomes as well. Table 2 shows a smaller decline in EU Macro

Table 4. Import and User Price Changes in the EU

Scenario		Import Prices		User Prices		Consumer
		Flat	Long	Flat	Long	Price Index
A.	Cap	0.69	-0.26	19.88	8.70	0.02
B.	M-BCA	37.10	29.90	34.58	16.36	0.04
C.	R-BCA	10.95	5.70	24.18	10.49	0.02
D.	DM-BCA	13.80	11.47	25.61	11.85	0.03

Notes: Values represent percentage changes relative to the benchmark. Import prices refer to the cost of imported steel products into the EU. User prices refer to the prices paid by end consumers within the EU. Consumer Price Index refers to the overall consumer price index within the EU.

Table 5. US Price Impacts of rate-based vs. Mass-based BCAs at Varying Stringency

Stringency	Flat		Long		Consumer	
	R-BCA	DM-BCA	R-BCA	DM-BCA	R-BCA	DM-BCA
Low	0.02	0.38	0.30	0.34	0.0001	-0.0021
Medium	0.65	1.05	1.60	0.94	0.0020	-0.0020
High	3.56	1.40	2.95	1.23	0.0081	-0.0019

Notes: Values represent percentage changes relative to the benchmark. Comparison is between US rate-based BCA and an environmentally equivalent discounted mass-based BCA. The Low, Medium, and High stringency levels correspond to the carbon prices in the EU M-BCA scenario at 10%, 30%, and 50% domestic emissions reduction targets, respectively (approximately \$20, \$88, and \$241 per ton CO_2).

Production under the rate-based scenario, by about one-third relative to the mass-based scenario (-0.081% versus -0.126%). At the same time, domestic steel output declines more under the rate-based design; for long steel, the decline is about 35% larger (-6.19% versus -4.60%), because lower-cost imports exert greater competitive pressure on domestic integrated mills. This is precisely the industrial-incidence trade-off in Proposition 5: the rate-based design protects downstream users by weakening protection for domestic upstream producers.

ASYMMETRIC CASE.—Finally, Table 5 shows that downstream protection under a rate-based design exhibits diminishing returns. In the US context, the rate-based instrument appears attractive at low stringency, minimizing welfare losses relative to a full tariff. But this advantage erodes as climate ambition rises: at low stringency, the rate-based design modestly cushions prices relative to the discounted mass-based benchmark, while at high stringency the flat-steel price increase is more than two and a half times as large (3.56% versus 1.40%). The reversal occurs because the rate-based design lacks a revenue margin. A mass-based tariff generates fiscal revenue that can be recycled to offset distortions, whereas a rate-based standard does not. The comparison again highlights that instrument choice governs not just environmental performance, but also how protection is allocated as ambition increases.

E. Sensitivity and Robustness

Finally, we ask whether our central findings are robust across different parameterizations and trace how specific parameters drive the underlying mechanisms. The quantitative results rely on the nested CES structure and its calibrated elasticities. Our baseline parameterization is empirically anchored by the micro-data variance presented in Table 1 of Section IV.C. For instance, the tightly clustered BOF operating practices justify near-Leontief plant-level rigidities (σ_a, σ_v^{Iron}), while the high variance in EAF scrap usage provides an empirical basis for greater flexibility in secondary production ($\sigma_{\text{EAF}}^{\text{Mat}}$). For macro-level parameters where micro-data is less prescriptive, such as Armington substitution elasticities (σ^A) and scrap supply elasticity (η_{Scrap}), we test wide bounds—typically scaling the baseline values by a factor of 0.5 and 2.0—to ensure our findings are not

artifacts of these choices.

The sensitivity analysis confirms that the core efficiency ranking is structurally robust across all parameterizations. Table C5 and Figure C4 demonstrate that the cost-effectiveness advantage of the mass-based design holds regardless of technological substitution limits or scrap availability. Quantitatively, global emissions reductions under the mass-based BCA remain tightly bounded between 1.29% and 1.39%, consistently outperforming the rate-based design, which is constrained to 0.87%–1.11% abatement. Furthermore, the regional welfare cost required to achieve a unit of global abatement remains significantly higher under the rate-based architecture across the entire parameter space.

Tracing the specific mechanisms confirms that vertical leakage is not a calibration artifact but a bounded structural outcome. As shown in Figure C3 and Table C6, the volume of vertical leakage—the surge in merchant pig iron imports under the rate-based design—is highly sensitive to the EAF material substitution elasticity ($\sigma_{\text{EAF}}^{\text{Mat}}$). However, the design's overall performance remains robust: global leakage rates under the mass-based BCA are bounded between 13% and 19%, consistently lower than the 31%–45% observed under the rate-based architecture. This aligns with physical intuition: the extent to which upstream emissions spike depends directly on the technical flexibility of secondary producers to substitute scrap with under-priced merchant iron. Because our plant-level data confirms that EAFs possess this operational flexibility, aggressive vertical leakage is a robust prediction of the intensity-gap incentive.

Finally, Table C7 highlights how key parameters govern abatement channels. The technique effect ranges from 1.93 to 4.41 Mt, driven by technological substitution limits (σ_a^{KLE}) and material flexibility ($\sigma_{\text{EAF}}^{\text{Mat}}$), which define the technological slack available for within-plant abatement. Conversely, the composition effect, shifting between -2.51 and -5.06 Mt, is moderated by scrap supply elasticity (η_{Scrap}), reflecting a resource bottleneck where limited scrap supply constrains the shift toward cleaner production. Despite these variations, the scale effect under the rate-based policy persists as a large positive emissions source. The fundamental inefficiency of the rate-based BCA, specifically its failure to compress demand due to an implicit output subsidy, is structurally robust across all parameter variations.

VI. Conclusions

This paper proposes and evaluates an economic framework for a fundamental choice in BCA design: whether border charges should price the full embodied emissions of imports or only emissions above an intensity benchmark. In a plant-level multi-region equilibrium model of the global steel industry, we show that a rate-based BCA operates as an emissions charge plus an implicit output subsidy. That wedge dilutes the carbon signal transmitted abroad. In the EU-style symmetric setting, the rate-based design transmits only 36% of the mass-based border price needed to deliver the same global emissions reduction and does so at higher welfare cost. In the US-style asymmetric setting, where no domestic carbon price anchors the border instrument, the effective signal falls to about one-eighth and the policy mainly reallocates scarcity rents rather than inducing abatement abroad.

Because steel combines large dispersion in embodied emissions with explicit trade in carbon-intensive intermediates, the margins through which adjustment occurs are central to policy evaluation. Benchmark-based BCAs create scope for both reshuffling and vertical leakage. In our quantitative results, the rate-based design more than doubles EU pig iron imports relative to the mass-based alternative and shifts foreign adjustment away from the scale margin toward composition responses. Models that omit plant heterogeneity or vertical linkages are therefore likely to overstate the environmental performance of benchmark-based BCAs. To the extent that other EITE sectors share these features, the same concern extends beyond steel.

This paper calls attention to interactions between two issues that policy debates often treat separately: how much climate ambition a BCA transmits abroad and how protection is allocated across regions and along the supply chain. These results imply that BCA architecture and domestic carbon pricing are complements, not substitutes. Where a domestic carbon price already exists, a border measure can extend that signal abroad, but the choice of architecture determines how much ambition is transmitted and where protection is allocated within the supply chain. Where no domestic price anchor exists, especially under a rate-based design, border measures mainly redistribute protection. Taken together, the results point to a design principle rather than a one-size-fits-all ranking. Rate-based BCAs are most vulnerable where the industry combines rigid upstream stages with benchmarkable but weakly responsive emissions intensities; in such settings, stronger price signals are needed to prevent arbitrage and vertical leakage. By contrast, the case for rate-based designs is stronger in heterogeneous downstream products, where technology choice is more responsive and the political value of downstream price protection is greater. This points to a case for product-specific design: mass-based treatment may be more appropriate for homogeneous upstream intermediates, while a rate-based design may be more attractive in heterogeneous downstream products. A consumption-based charge or climate contribution could also be paired with a rate-based BCA to restore the scale effect and generate revenue for recycling while preserving targeted technology incentives.

Three questions seem especially important for future work. First, how much do our static results understate the long-run technique margin? Work on industry dynamics under market-based environmental policy shows that investment, technology adoption, and entry can materially change policy incidence and efficiency (Fowlie, Reguant and Ryan, 2016). In the BCA context, an open question is whether the stronger dynamic incentives sometimes associated with benchmark- based instruments can offset the weaker static scale incentives emphasized in this paper.

Second, how does BCA architecture shape strategic responses across jurisdictions? Recent work studies BCAs as part of broader climate-club and international-coordination problems (Nordhaus, 2015; Clausing and Wolfram, 2023; Beaufils, Wanner and Wenz, 2024). Our results suggest that architecture affects not only leakage and competitiveness, but also where scarcity rents accrue along the supply chain. Whether these incidence effects make some BCA designs more conducive to reciprocal carbon pricing, retaliation, or coalition formation remains an open question.

Third, how far do these mechanisms extend beyond steel? A growing literature shows that firm heterogeneity and input-output linkages can be central for the effects of unilateral climate policy and border measures (Sogalla, 2025; Stillger, 2025; Clausing et al., 2025). But EITE sectors differ in technological dispersion, the tradability of intermediates, and the location of political pressure. Identifying when the steel logic carries over to aluminum, cement, chemicals, and other sectors is therefore an important avenue for future work.

REFERENCES

Abrell, Jan, Sebastian Rausch, and Clemens Streitberger. 2019. "The Economics of Renewable Energy Support." *Journal of Public Economics*, 176: 94–117.

Aguiar, Angel, Maksym Chepeliev, Erwin Corong, and Dominique Van Der Mensbrugghe. 2022. "The Global Trade Analysis Project (GTAP) Data Base: Version 11." *Journal of Global Economic Analysis*, 7(2): 1–37.

Akerman, Anders, Rikard Forslid, and Ossian Prane. 2024. "Imports and the CO2 Emissions of Firms." *Journal of International Economics*, 152: 104004.

Anderson, James E., and Eric van Wincoop. 2003. "Gravity with Gravitas: A Solution to the Border Puzzle." *American Economic Review*, 93(1): 170–192.

Beaufils, Timothé, Joschka Wanner, and Leonie Wenz. 2024. "The Potential of Carbon Border Adjustments to Foster Climate Cooperation."

Ben-David, Itzhak, Yeejin Jang, Stefanie Kleimeier, and Michael Viehs. 2021. "Exporting Pollution: Where Do Multinational Firms Emit CO2?" *Economic Policy*, 36(107): 377–437.

Böhringer, Christoph, Edward J. Balistreri, and Thomas F. Rutherford. 2012. "The Role of Border Carbon Adjustment in Unilateral Climate Policy: Overview of an Energy Modeling Forum Study (EMF 29)." *Energy Economics*, 34: S97–S110.

BP. 2022. "Statistical Review of World Energy 2022."

Brunel, Claire, and Arik Levinson. 2024. "Carbon Tariffs 101." National Bureau of Economic Research w33024.

Campolmi, Alessia, Harald Fadinger, Chiara Forlati, Sabine Stillger, and Ulrich J. Wagner. 2025. "Designing Effective Carbon Border Adjustment with Minimal Information Requirements. Theory and Evidence." Social Science Research Network SSRN Scholarly Paper 4644941.

Clausing, Kimberly A., and Catherine Wolfram. 2023. "Carbon Border Adjustments, Climate Clubs, and Subsidy Races When Climate Policies Vary." *Journal of Economic Perspectives*, 37(3): 137–162.

Clausing, Kimberly, Jonathan Colmer, Allan Hsiao, and Catherine Wolfram. 2025. "The Global Effects of Carbon Border Adjustment Mechanisms." National Bureau of Economic Research w33723.

Cohen, Francois, and Giulia Valacchi. 2022. "The Heterogeneous Impact of Coal Prices on the Location of Cleaner and Dirtier Steel Plants." *The Energy Journal*, 43(2): 67–90.

Collard-Wexler, Allan, and Jan De Loecker. 2015. "Reallocation and Technology: Evidence from the US Steel Industry." *American Economic Review*, 105(1): 131–171.

Copeland, Brian R. 1996. "Pollution Content Tariffs, Environmental Rent Shifting, and the Control of Cross-Border Pollution." *Journal of International Economics*, 40(3-4): 459–476.

Copeland, Brian R., and M. Scott Taylor. 2004. "Trade, Growth, and the Environment." *Journal of Economic Literature*, 42(1): 7–71.

Coster, Pierre, Isabelle Mejean, and Julian di Giovanni. 2024. "Firms' Supply Chain Adaptation to Carbon Taxes."

Costinot, Arnaud, and Andrés Rodríguez-Clare. 2014. "Trade Theory with Numbers: Quantifying the Consequences of Globalization." In *Handbook of International Economics*. Vol. 4, , ed. Gita Gopinath, Elhanan Helpman and Kenneth Rogoff, 197–261. Elsevier.

CRU Group. 2023. "CRU Steel Cost Service."

Dechezleprêtre, Antoine, Caterina Gennaioli, Ralf Martin, Mirabelle Muûls, and Thomas Stoerk. 2022. "Searching for Carbon Leaks in Multinational Companies." *Journal of Environmental Economics and Management*, 112: 102601.

Duscha, Vicki, Everett B. Peterson, Joachim Schleich, and Katja Schumacher. 2019. "Sectoral Targets to Address Competitiveness – a CGE Analysis with Focus on the Global Steel Sector." *Climate Change Economics*, 10(01): 1950001.

Eaton, Jonathan, and Samuel Kortum. 2002. "Technology, Geography, and Trade." *Econometrica*, 70(5): 1741–1779.

European Steel Association. 2020. "Successful Implementation of Bold New 2030 Climate Target Urgently Needs Tangible Framework." *Press release*.

Farrokhi, Farid, and Ahmad Lashkaripour. 2025. "Can Trade Policy Mitigate Climate Change?" *Econometrica*, 93(5): 1561–1599.

Felbermayr, Gabriel, Sonja Peterson, and Joschka Wanner. 2025. "Trade and the Environment, Trade Policies and Environmental Policies—How Do They Interact?" *Journal of Economic Surveys*, 39(3): 1148–1184.

Fischer, Carolyn, and Alan K. Fox. 2012. "Comparing Policies to Combat Emissions Leakage: Border Carbon Adjustments versus Rebates." *Journal of Environmental Economics and Management*, 64(2): 199–216.

Fontagné, Lionel, and Katheline Schubert. 2023. "The Economics of Border Carbon Adjustment: Rationale and Impacts of Compensating for Carbon at the Border." *Annual Review of Economics*, 15(1): 389–424.

Fowlie, Meredith, Claire Petersen, and Mar Reguant. 2021. "Border Carbon Adjustments When Carbon Intensity Varies across Producers: Evidence from California." *AEA Papers and Proceedings*, 111: 401–405.

Fowlie, Meredith, Mar Reguant, and Stephen P. Ryan. 2016. "Market-Based Emissions Regulation and Industry Dynamics." *Journal of Political Economy*, 124(1): 249–302.

Fullerton, Don, and Gilbert E. Metcalf. 2001. "Environmental Controls, Scarcity Rents, and Pre-Existing Distortions." *Journal of Public Economics*, 80(2): 249–267.

Global Energy Monitor. 2023. "Global Steel Plant Tracker."

Goulder, Lawrence H., Marc A. C. Hafstead, and Roberton C. Williams III. 2016. "General Equilibrium Impacts of a Federal Clean Energy Standard." *American Economic Journal: Economic Policy*, 8(2): 186–218.

Hertel, Thomas W., ed. 1997. *Global Trade Analysis: Modeling and Applications*. Cambridge University Press.

Holland, Stephen P. 2012. "Emissions Taxes versus Intensity Standards: Second-Best Environmental Policies with Incomplete Regulation." *Journal of Environmental Economics and Management*, 63(3): 375–387.

Holland, Stephen P., Jonathan E. Hughes, and Christopher R. Knittel. 2009. "Greenhouse Gas Reductions under Low Carbon Fuel Standards?" *American Economic Journal: Economic Policy*, 1(1): 106–146.

Itskhoki, Oleg, and Dmitry Mukhin. 2025. "The Optimal Macro Tariff." National Bureau of Economic Research w33839.

Keen, Michael, and Christos Kotsogiannis. 2014. "Coordinating Climate and Trade Policies: Pareto Efficiency and the Role of Border Tax Adjustments." *Journal of International Economics*, 94(1): 119–128.

Keen, Michael, and Christos Kotsogiannis. 2025. "Principles for Pareto Efficient Border Carbon Adjustment."

Kortum, Samuel, and David Weisbach. 2026. "Regional Carbon Policy in a Global Economy."

Mathiesen, Lars, and Ottar Mæstad. 2004. "Climate Policy and the Steel Industry: Achieving Global Emission Reductions by an Incomplete Climate Agreement." *The Energy Journal*, 25(4): 91–114.

Nordhaus, William. 2015. "Climate Clubs: Overcoming Free-Riding in International Climate Policy." *American*

Economic Review, 105(4): 1339–70.
OECD. 2021. "OECD Inter-Country Input-Output Database."
OECD. 2024*a*. "International Transport and Insurance Costs of Merchandise Trade (ITIC)."
OECD. 2024*b*. "Structural and Demographic Business Statistics (SDBS)."
OECD. 2024*c*. "Trade by Enterprise Characteristics (TEC)."
Pizer, William A., and Erin Campbell. 2021. "Border Carbon Adjustments without Full (or Any) Carbon Pricing." Resources for the Future 21-21.
Rutherford, Thomas F. 1995. "Extension of GAMS for Complementarity Problems Arising in Applied Economic Analysis." *Journal of Economic Dynamics and Control*, 19(8): 1299–1324.
Shapiro, Joseph S., and Reed Walker. 2018. "Why Is Pollution from US Manufacturing Declining? The Roles of Environmental Regulation, Productivity, and Trade." *American Economic Review*, 108(12): 3814–54.
Sogalla, Robin. 2025. "Unilateral Carbon Pricing and Heterogeneous Firms."
Sogalla, Robin, Joschka Wanner, and Yuta Watabe. 2024. "New Trade Models, Same Old Emissions?" Deutsches Institut für Wirtschaftsforschung (DIW) DIW Discussion Papers 2077.
Stillger, Sabine. 2025. "The Role of Firm Heterogeneity and Intermediate Inputs in Carbon Leakage."
United Nations Statistics Division. 2024. "UN Comtrade Database."
U.S. Energy Information Administration. 2024. "International Energy Statistics."
van der Mensbrugghe, Dominique. 2019. "The Standard GTAP Model in GAMS, Version 7.1." Center for Global Trade Analysis, Purdue University GTAP Technical Paper 6825.
Weisbach, David A., Samuel Kortum, Michael Wang, and Yujia Yao. 2023. "Trade, Leakage, and the Design of a Carbon Tax." *Environmental and Energy Policy and the Economy*, 4: 43–90.
World Steel Association. 2016. "Top Steel-Producing Companies 2015."
World Steel Association. 2018. "Top Steelmakers in 2017."
World Steel Association. 2020. "Top Steelmakers in 2019."
World Steel Association. 2022. "Steel Statistical Yearbook 2022."
World Steel Association. 2023. "World Steel in Figures 2023."

Environmental Ambition and Economic Protectionism: The Design of Border Carbon Adjustments

Online Appendix

Eunseong Park, Sebastian Rausch, and Valerie J. Karplus

Contents:

A. Formal Proofs

This appendix provides the formal mathematical derivations for the lemmas and propositions presented in the Conceptual Framework (Section II).

A1. Proof of Lemma 1 (Price Ranking)

PROOF: The equilibrium price is the sum of production costs and the border charge: $p_{i,h} = c(s_{c,i}) + t(\epsilon_{i,h})$. Under a mass-based design, $t^M(\epsilon) = \tau\epsilon_{i,h}$. Under a rate-based design, $t^R(\epsilon) = \tau(\epsilon_{i,h} - \bar{\psi})$. We can express the rate-based charge as a fraction of the mass-based charge:

$$t^R = \tau\epsilon_{i,h}\left(1 - \frac{\bar{\psi}}{\epsilon_{i,h}}\right) = \lambda\tau\epsilon_{i,h} \tag{A1}$$

where $\lambda = (1 - \bar{\psi}/\epsilon_{i,h})$. Since $\bar{\psi} > 0$ and $\epsilon_{i,h} > 0$ for carbon-intensive varieties, then $\lambda < 1$. The price ranking follows directly:

$$p^M_{i,h} - p^R_{i,h} = \tau\epsilon_{i,h} - \lambda\tau\epsilon_{i,h} = \tau\bar{\psi} > 0 \tag{A2}$$

Thus, $p^M_{i,h} > p^R_{i,h}$. In the symmetric paradigm, λ represents the dilution of the domestic price anchor. In the asymmetric paradigm, λ represents the effective stringency relative to a mass-based reference price.

A2. Proof of Proposition 1 (Global Cost-Effectiveness)

PROOF: A cost-effective achievement of the global target $\bar{E}$ requires minimizing the sum of production costs and lost consumer value for a given emissions constraint. Let Q^M and Q^R denote the equilibrium demand for the composite intermediate Q under the mass-based and rate-based designs, respectively. In a competitive equilibrium, the mass-based design internalizes the carbon constraint on both the technology adoption margin ($s_{c,i}$) and the consumption margin (Q), thereby achieving the cost-effective benchmark $Q^M = Q^*$.

The cost-effectiveness conditions require that the marginal cost of technology adoption equals the marginal cost of reducing consumption:

$$\frac{c'(s_{c,i})}{-\epsilon'(s_{c,i})} = \frac{G'(Q)}{\epsilon(s_{c,i})} = \tau \tag{A3}$$

Under a rate-based BCA, the implicit subsidy $\sigma = \tau\bar{\psi}$ reduces the price index $P(p_{h,h}, p_{f,h})$ relative to the mass-based baseline. Consequently, downstream firms choose a larger volume $Q^R > Q^*$, neutralizing the consumption margin as a channel for abatement.

To satisfy the fixed global budget $\bar{E}$ at this larger scale, the sectoral intensity $\epsilon(s_c)$ must fall further than under the cost-effective benchmark, requiring a higher marginal carbon signal $\tau^R > \tau^M$. Since $c'' > 0$, the marginal cost of this additional technology switching is strictly higher than the marginal cost of the avoided consumption reduction. This results in a deadweight loss, as the total economic cost of achieving the target $\bar{E}$ is higher under the rate-based architecture.

A3. Proof of Proposition 2 (Foreign Composition–Scale Substitution)

PROOF: By construction, we compare two policy designs that achieve the same global emissions target $\bar{E}_{global} = E_h + E_f$. Given a fixed domestic emissions target $\bar{E}_h$ is achieved

in both scenarios, the foreign sector must satisfy a fixed residual emissions budget:

$$E_f = \epsilon_{f,h} q_{f,h} + \epsilon_{f,f} q_{f,f} = \bar{E}_f \tag{A4}$$

where $\bar{E}_f = \epsilon_f q_f$ is the sectoral emissions budget and $q_f = q_{f,h} + q_{f,f}$ is the total production volume.

From Lemma 1, the rate-based design results in a lower price index for the regulated variety ($p^R_{f,h} < p^M_{f,h}$) for any level of technological composition. For designs of equivalent stringency, the rate-based instrument sustains a larger trade volume $q^R_{f,h} > q^M_{f,h}$. Focusing on the benchmark case of inelastic foreign domestic demand established in the Setup, this implies a larger total production scale: $q^R_f > q^M_f$. This result is robust to elastic foreign domestic demand as long as the expansion of trade volume—enabled by the intensity benchmark—outweighs the contraction of the foreign domestic market caused by higher regional production costs.

To satisfy the fixed emissions budget $\bar{E}_f$, the higher production scale q^R_f must be offset by a lower average sectoral intensity ϵ^R_f:

$$\epsilon^R_f = \frac{\bar{E}_f}{q^R_f} < \frac{\bar{E}_f}{q^M_f} = \epsilon^M_f \tag{A5}$$

Given the intensity definition $\epsilon_f = s_{c,f}\epsilon_c + (1 - s_{c,f})\epsilon_d$, the lower sectoral intensity $\epsilon^R_f < \epsilon^M_f$ necessitates a strictly higher clean technology share $s^R_{c,f} > s^M_{c,f}$. This formalizes the fundamental trade-off: by neutralizing the scale margin as an abatement channel, the rate-based design forces the foreign sector to rely more heavily on the composition margin to achieve a given environmental outcome.

A4. Proof of Lemma 2 (Reshuffling Priority)

PROOF: The foreign producer allocates production from a technology portfolio $\{q_c, q_d\}$ to two markets $\{h, f\}$. The producer minimizes total tax-inclusive costs:

$$\min \sum_{j \in \{h,f\}} [c(s_{c,j}) q_j + t(\epsilon_j) q_j \cdot \mathbb{I}_{j=h}] \tag{A6}$$

subject to $\sum_j q_{c,j} \leq q_c$ and $\sum_j q_{d,j} \leq q_d$. The first-order condition for allocating a clean unit to market h versus f yields a tax-saving term $\tau(\epsilon_d - \epsilon_c)$ that is strictly positive. Since costs are otherwise identical across markets, the producer will always prioritize the clean variety for the export market h to minimize the border charge.

A5. Proof of Proposition 3 (Reshuffling and Capacity Pressure)

PROOF: Consider a comparison between a rate-based and a mass-based design at the same marginal carbon price τ_f. Let $q_f = q_{f,h} + q_{f,f}$ be the total foreign production. By Lemma 2, producers prioritize the allocation of clean units to the regulated market. The observed intensity at the border, $\epsilon_{f,h}$, is the weighted average of the intensities of the clean ($q_{c,f,h}$) and dirty ($q_{d,f,h}$) units allocated to the export market:

$$\epsilon_{f,h} = \frac{q_{c,f,h}\epsilon_c + (q_{f,h} - q_{c,f,h})\epsilon_d}{q_{f,h}} \tag{A7}$$

Solving for the volume of clean units required to hit the target $\bar{\psi}_{f,h}$ yields:

$$q_{c,f,h} = q_{f,h}\left[\frac{\epsilon_d - \bar{\psi}_{f,h}}{\epsilon_d - \epsilon_c}\right] \tag{A8}$$

From Lemma 1, the rate-based design results in a lower price for the variety sold in the regulated market ($p^R_{f,h} < p^M_{f,h}$), which sustains a larger export volume $q^R_{f,h} > q^M_{f,h}$. At this higher export scale, the existing clean capacity $s_{c,f}q_f$ is diluted over a larger volume, making it more difficult to achieve the intensity target $\psi_{f,h}$ through reshuffling alone.

To maintain the target $\bar{\psi}_{f,h}$ at the larger scale $q^R_{f,h}$, the required absolute clean production $q^R_{c,f,h}$ must satisfy:

$$q^R_{c,f,h} = q^R_{f,h}\left[\frac{\epsilon_d - \bar{\psi}_{f,h}}{\epsilon_d - \epsilon_c}\right] > q^M_{f,h}\left[\frac{\epsilon_d - \bar{\psi}_{f,h}}{\epsilon_d - \epsilon_c}\right] = q^M_{c,f,h} \tag{A9}$$

Since the total volume of clean units must satisfy $s_{c,f}q_f \geq q_{c,f,h}$, the larger requirement $q^R_{c,f,h}$ necessitates an expansion of the total regional clean technology share $s_{c,f}$ in the foreign sector. Thus, by preserving trade scale, the rate-based design creates capacity pressure that forces deeper technology adoption to compensate for the dilution of reshuffled assets.

A6. Proof of Proposition 4 (Regional Incidence and Terms-of-Trade)

PROOF: Let regional welfare be defined as the sum of producer surplus, downstream surplus, and fiscal revenue. Considering the impact of the border adjustment on Home welfare W_h and Foreign welfare W_f:

$$W_h = \Pi_{u,h} + \Pi_d + R_{BCA} \tag{A10}$$

$$W_f = \Pi_{u,f} \tag{A11}$$

where R_{BCA} is the fiscal revenue collected at the border. Under a mass-based design, $R^M_{BCA} = \tau_f \epsilon_{f,h} q_{f,h}$. Under a rate-based design, the intensity benchmark $\bar{\psi}$ creates an implicit subsidy $\sigma = \tau_f \bar{\psi}$, such that $R^R_{BCA} = \tau_f(\epsilon_{f,h} - \bar{\psi})q_{f,h} = R^M_{BCA} - \sigma q_{f,h}$.

The difference in fiscal revenue collected by the Home government, $R^M_{BCA} - R^R_{BCA} = \sigma q_{f,h}$, constitutes a direct transfer of economic surplus to the Foreign export sector. Because the rate-based design lowers the effective border charge (Lemma 1), it increases Foreign producer surplus ($\Pi^R_{u,f} > \Pi^M_{u,f}$) and domestic downstream surplus ($\Pi^R_d > \Pi^M_d$). However, this gain for the downstream sector is offset by the loss of fiscal revenue. For a sufficiently small downstream value-added, $W^M_h > W^R_h$, as the mass-based design maximizes the extraction of scarcity rents from foreign producers, thereby improving the regional terms-of-trade.

A7. Proof of Proposition 5 (Industrial Incidence)

PROOF: Let $\Pi_{u,h}$ denote the producer surplus of domestic upstream producers, which is strictly increasing in the price of the competing imported variety $p_{f,h}$. From Lemma 1, $p^M_{f,h} > p^R_{f,h}$, which implies higher surplus for domestic producers under the mass-based design: $\Pi_{u,h}(p^M_{f,h}) > \Pi_{u,h}(p^R_{f,h})$.

For the downstream sector, the surplus is $\Pi_d = \max_Q\{G(Q) - PQ\}$, representing the value-added accruing to fixed factors in downstream production. By the Envelope Theo-

rem:

$$\frac{d\Pi_d}{dP} = -Q(P) < 0 \tag{A12}$$

Since the dual price index P is increasing in input prices, $P(p_{h,h}, p^M_{f,h}) > P(p_{h,h}, p^R_{f,h})$. Therefore, downstream surplus is strictly higher under the rate-based design:

$$\Pi_d(P^R) > \Pi_d(P^M) \tag{A13}$$

A8. Proof of Proposition 6 (Reshoring and Diluted Abatement)

PROOF: Total global emissions are defined as $E_{global} = \epsilon_{h,h} q_{h,h} + \epsilon_{f,h} q_{f,h} + \epsilon_{f,f} q_{f,f}$, where $\epsilon_{f,h}$ and $\epsilon_{f,f}$ denote the average intensities of foreign production allocated to the regulated and unregulated markets, respectively. Differentiating with respect to the border charge t:

$$\frac{dE_{global}}{dt} = \underbrace{(\epsilon_{h,h} - \epsilon_{f,h})\frac{dq_{h,h}}{dt}}_{\text{Substitution Effect}} + \underbrace{q_{f,h}\frac{d\epsilon_{f,h}}{dt} + q_{f,f}\frac{d\epsilon_{f,f}}{dt}}_{\text{Abatement/Reshuffling Effect}} \tag{A14}$$

With $\tau_h = 0$, domestic intensity $\epsilon_{h,h}$ is constant. Since the BCA raises the price of the foreign variety, $\frac{dq_{h,h}}{dt} > 0$ (reshoring). If domestic production is dirtier than the foreign imports ($\epsilon_{h,h} > \epsilon_{f,h}$), the substitution effect is positive. While the foreign producer may clean up its exports ($\frac{d\epsilon_{f,h}}{dt} < 0$), if this cleanup is achieved primarily through reshuffling existing units from the domestic to the export market rather than sectoral investment ($s_{c,f}$), then $d\epsilon_{f,f}/dt > 0$, and the net global abatement is diminished.

A9. Proof of Lemma 3 (Homogeneous Sectors)

PROOF: In a rate-based design, the implicit marginal penalty δ^R is determined by the aggregate sectoral compliance condition: $\sum_i \bar{\psi} q_{i,h} = \sum_i \epsilon_{i,h} q_{i,h}$, which requires the aggregate sectoral intensity to equal the benchmark ($\bar{\epsilon} = \bar{\psi}$). Substituting the intensity definition $\epsilon_{i,h} = s_{c,i,h}\epsilon_c + (1 - s_{c,i,h})\epsilon_d$:

$$\bar{\epsilon} = \epsilon_d - s_{c,i,h}(\epsilon_d - \epsilon_c) = \bar{\psi} \tag{A15}$$

Solving for the required clean technology share $s_{c,i,h}$ yields:

$$s^*_{c,i,h} = \frac{\epsilon_d - \bar{\psi}}{\epsilon_d - \epsilon_c} \tag{A16}$$

As $\epsilon_c \to \epsilon_d$, the denominator approaches zero. If $\bar{\psi}$ is set below the physical limit of the technology ($\bar{\psi} < \epsilon_c \approx \epsilon_d$), the required share $s^*_{c,i,h}$ becomes mathematically undefined and exceeds 1, indicating that the target cannot be met at any price ($\delta^R \to \infty$). Conversely, if $\bar{\psi} > \epsilon_c \approx \epsilon_d$, the condition is always satisfied even at $s_{c,i,h} = 0$, causing the implicit penalty to collapse to zero ($\delta^R = 0$). Thus, the effective border penalty exhibits a knife-edge sensitivity to the benchmark level in homogeneous sectors.

A10. Proof of Proposition 7 (Vertical Leakage)

PROOF: The price of the intermediate input in the domestic market for a domestic producer h is $p_h = c(s_{c,h}) + \tau_h \epsilon_h$. For a foreign producer f, the price inclusive of the border adjustment is $p_{f,h} = c(s_{c,f}) + t(\epsilon_f)$.

From Lemma 3, if the intermediate sector is homogeneous, $t(\epsilon_f) \approx 0$. Assuming production costs $c(\cdot)$ and intensities ϵ are approximately equal across regions for the homogeneous input, the resulting price wedge $\Delta p = p_h - p_{f,h}$ is:

$$\Delta p \approx [c(s) + \tau_h \epsilon] - [c(s) + 0] = \tau_h \epsilon \tag{A17}$$

The domestic producer faces a competitive disadvantage equal to the full domestic carbon cost $\tau_h \epsilon$. Downstream firms, seeking to minimize the price index $P(p_h, p_{f,h})$, will substitute the domestic intermediate with imports $q_{f,h}$, shifting the emissions-intensive stage of production offshore.

B. Data Construction

This appendix details the construction of the global dataset, which harmonizes plant-level engineering estimates with aggregate trade and production statistics. The procedure ensures that the micro-level heterogeneity in technology and efficiency is preserved while satisfying macro-level constraints on global supply and demand.

B1. Data Sources and Sample Selection

The core iron and steel production data is drawn from the CRU Steel Cost Service for the baseline year 2019 (CRU Group, 2023). We extract key physical and economic parameters for each facility, including production capacities, operating rates, granular material inputs (e.g., kg per tonne of output), energy consumption vectors, and local unit costs for factors of production.

We apply a rigorous data cleaning and validation protocol to clean and harmonize the raw data. Plants are excluded if they report discontinuous operations, missing vital cost components, or negligible sales volumes (defined as less than 0.1 kt annually). Following the plant-level filtering, we map individual ISO-alpha3 country codes from plant locations into the model's distinct custom regions (e.g., USA, China, EU28/EFTA, Russia/CIS/Ukraine, and rest of world aggregates). This mapping balances computational tractability with the resolution required for accurate policy evaluation. We validate the representativeness of this cleaned sample by cross-referencing aggregate regional capacities against the Global Steel Plant Tracker (GSPT) and production totals against the World Steel Association (worldsteel) (Global Energy Monitor, 2023; World Steel Association, 2022).

B2. Process Modeling and Carbon Accounting

Translating engineering cost accounts into economic production functions requires two major structural adjustments. First, we map granular sub-processes into the model's aggregated sectors. We incorporate the physical and economic profiles of upstream activities—specifically blast furnace pelletizing, direct reduction (DR) pelletizing, coke making, and sintering—and consolidate their costs and physical inputs recursively into the primary ironmaking functions (blast furnace, DRI, Corex, and custom ironmaking). Specific configurations, such as Conarc and custom iron or steelmaking setups, are standardized into representative BF or DRI functions. Crucially, the pipeline calculates net intermediate production to maintain mass-balance consistency. Pig iron and DRI outputs are dynamically split between captive consumption (used on-site for steelmaking) and merchant surplus (sold to third parties).

Second, we rigorously correct for byproducts to ensure accurate carbon accounting. Standard industry cost accounting frameworks typically treat process gases (e.g., blast furnace gas, coke oven gas) and surplus generated power or steam as revenue credits that artificially lower net operational costs. For a physical climate model, however, these must be treated as conserved energy flows to track emissions accurately. To resolve this, we calculate a mathematical correction factor ϕ^{bp} to convert these financial credits back into gross physical input requirements:

$$\phi^{bp} = 1 - \frac{\text{Total Production}}{\text{Total Consumption}} \tag{B1}$$

Here, "Total Consumption" refers to the absolute gross amount of an energy carrier a plant physically requires for its processes, while "Total Production" is the volume of that carrier the plant generates internally as a byproduct. The factor ϕ^{bp} calculates the

share of the required energy that must be purchased externally. Multiplying the gross input requirement by ϕ^{bp} yields the net physical external input, preventing the double-counting of emissions from self-generated process gases and ensuring the model captures the true energy intensity of production. We also calculate and add the auxiliary energy requirements for desulfurization and secondary steelmaking to the core process definitions to capture the full, unabated energy footprint of semi-finished steel products.

B3. Regional and Raw Material Balances

To reconcile the bottom-up microdata with official national accounts, we employ a systematic re-weighting procedure. Plant-level output is scaled to match authoritative worldsteel regional control totals for both intermediate inputs (pig iron, DRI) and final steel goods (flat and long products) (World Steel Association, 2022). We calculate a regional adjustment factor $\alpha_{r,s}$ for each region r and sector s:

$$\alpha_{r,s} = \frac{Y_{r,s}^{\text{worldsteel}}}{Y_{r,s}^{\text{CRU}}} \tag{B2}$$

where Y denotes aggregate production. Each plant's output is multiplied by this factor, ensuring that the baseline simulation exactly reproduces observed regional distinctives in production scale without altering the underlying micro-level cost distributions or technological shares.

For primary raw materials, we construct physically consistent global balances with differing approaches depending on data availability. For iron ore and ferrous scrap, total consumption (C) is determined bottom-up from CRU plant requirements, while bilateral trade flows (exports X and imports M) are anchored to UN Comtrade statistics (United Nations Statistics Division, 2024). Production (Y) is therefore derived as the residual ($Y = C + X - M$), with imports proportionally scaled down if they implausibly exceed total consumption. Missing Comtrade quantities are imputed using regional average prices. Natural gas bilateral trade (pipeline and liquefied natural gas) and production are sourced directly from the internally consistent BP Statistical Review (BP, 2022), with consumption calculated as the residual.

In contrast to gas and ore, the dataset isolates the trade of metallurgical (coking) coal rather than thermal coal. Regional production and consumption data for metallurgical coal are sourced from the U.S. Energy Information Administration (EIA) (U.S. Energy Information Administration, 2024), but consistent bilateral trade flows are unavailable at the same coverage. Therefore, we assume bilateral flows follow the general coal trade patterns (HS code 270112) from UN Comtrade (United Nations Statistics Division, 2024). To reconcile the discrepancies between the independent macroeconomic totals and the trade network, we frame the problem as a quadratic programming optimization. This minimizes the squared deviation from the reported EIA totals subject to the global material balance constraint ($Y_r + M_r = C_r + X_r$, and $\sum_r X_r = \sum_r M_r$). After finding the optimal balanced macro totals, we apply Iterative Proportional Fitting (IPF) to adjust the Comtrade bilateral matrix to exactly match these new targets.

B4. Trade Flow Imputation

Modeling trade with heterogeneous firms requires determining not just how much is traded between countries (intensive margin), but which specific plants participate in export markets (extensive margin). Since customs data (UN Comtrade) provides only aggregate bilateral flows (United Nations Statistics Division, 2024), we impute plant-level trade linkages for final steel products (flat and long steel) through a three-step procedure that combines structural gravity estimation with our micro-level cost data. Intermediate iron

products (pig iron and DRI) are allocated proportionally based on plant-level surplus production.

CALIBRATION OF EXPORTING MARGINS.—First, we calibrate the extensive margin—the share of firms in a region that export to a specific destination—using firm-level trade statistics from the OECD. We integrate multiple OECD datasets: Inter-Country Input-Output (ICIO) tables for trade flows (X_{ijs}), International Transport and Insurance Costs (ITIC) for CIF/FOB transport margins, Structural and Demographic Business Statistics (SDBS) for total firm counts (N_{iis}), and Trade by Enterprise Characteristics (TEC) for exporting firm counts (N_{is}) (OECD, 2021, 2024*a*,*b*,*c*). Following Sogalla, Wanner and Watabe (2024), we estimate a gravity regression to predict the destination-specific exporting firm share s_{ijs}:

$$\ln(s_{ijs}) = \beta_0 + \beta_1 \ln(\lambda_{ijs}) + \beta_2 \ln(\text{dist}_{ij}) + \gamma_j + \epsilon_{ij} \tag{B3}$$

where $\lambda_{ijs} = X_{ijs}/X_{iis}$ is the bilateral trade intensity, $\text{dist}_{ij} = 1/(1 - \text{ITIC}_{ij})$ is the transport cost friction, and γ_j are destination fixed effects. This estimation provides a region-pair specific target for the proportion of capacity that serves each export market.

RICARDIAN SELECTION.—Second, we identify the specific plants that fill these export quotas using a Ricardian selection mechanism. Consistent with trade theory, we assume that more productive (lower-cost) firms are more likely to overcome fixed trade costs. Within each region, we rank plants by their unit production costs $c_{i,a}$. We define an initial set of exporting plants $\mathcal{E}_{r,s,v}$ for each destination and variety by satisfying the discrete plant count quota $\lceil s_{r,s,v} N_{r,v} \rceil$ with the lowest-cost facilities. This ranking mechanism ensures that the model preserves the theoretical correlation between productivity and export participation observed in microdata.

BILATERAL FLOW RECONCILIATION.—Finally, we determine the plant-level trade flows $q_{i,s,a,v}$ using an iterative reconciliation procedure. For each plant in the exporting set $\mathcal{E}_{r,s,v}$, we calculate an initial sales volume $q^0_{i,s,a,v}$ based on its unit production cost $c_{i,a}$:

$$q^0_{i,s,a,v} = q^M_{r,s,v} \times \frac{c_{i,a}^{-(\sigma_v^M - 1)}}{\sum_{(k,a') \in \mathcal{E}_{r,s,v}} c_{k,a'}^{-(\sigma_v^M - 1)}} \tag{B4}$$

where $q^M_{r,s,v}$ is the aggregate bilateral trade volume and σ_v^M is the Armington substitution elasticity across foreign origins (see eq. 12). This weighting ensures structural consistency between the data imputation and the model's behavioral assumptions. We then apply the IPF procedure to adjust these flows until they simultaneously satisfy micro-level production constraints ($\sum_s q_{i,s,a,v} = q_{i,a,v}$) and macro-level trade totals ($\sum_{i \in \mathcal{I}_r} \sum_a q_{i,s,a,v} = q^M_{r,s,v}$). Crucially, if the IPF fails to converge for a specific region-variety pair, the model iteratively relaxes the extensive margin constraint by expanding the set $\mathcal{E}_{r,s,v}$ to include the next most efficient plants. This robust approach ensures that plant-level activity exactly reproduces the observed global trade network while maintaining the Ricardian sorting of firms.

C. Online Figures and Tables

(a) CRU Steel Cost Service (Number of production units: 311)

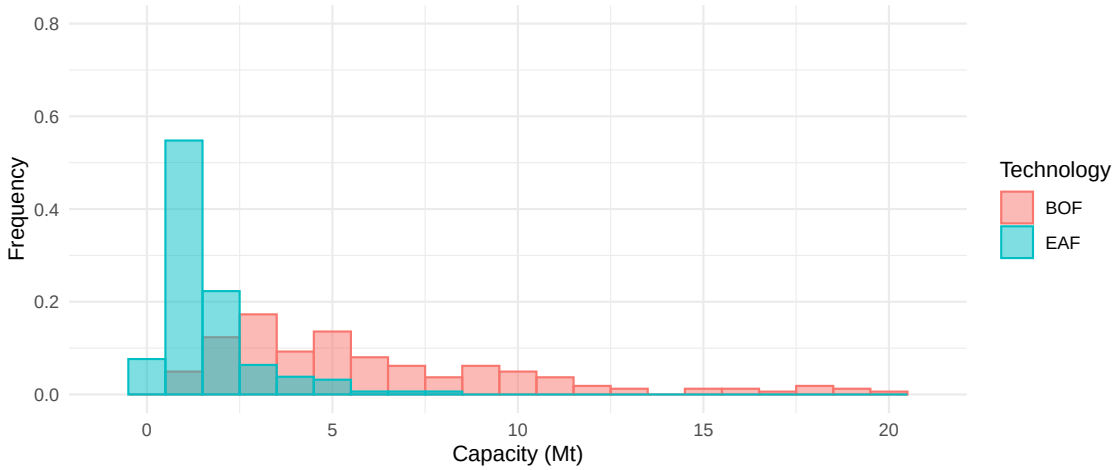

(b) Global Steel Plant Tracker (Number of production units: 932)

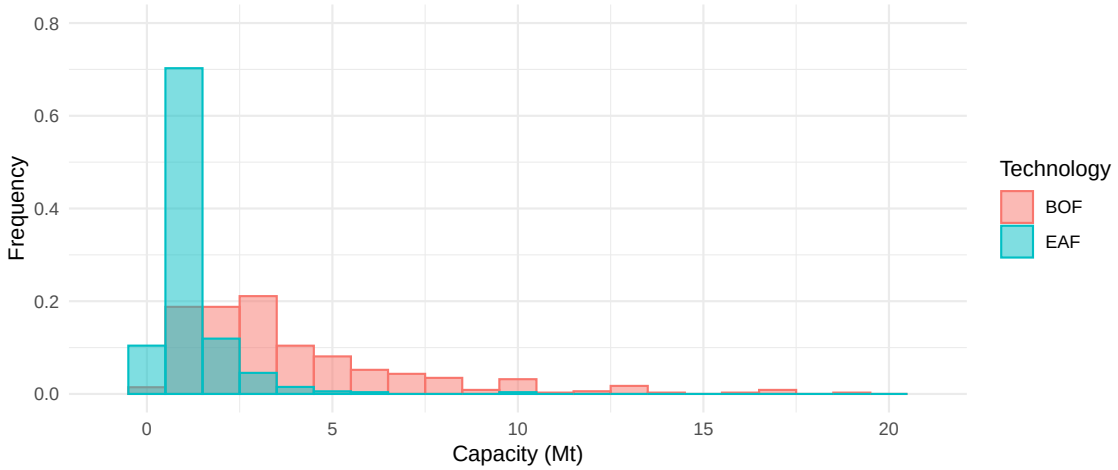

Figure C1. Histogram of Steel Plants by Production Capacity per Year

Notes: Panels show the distribution of plant capacities; sample sizes are reported in the panel captions. Source: CRU Steel Cost Service and Global Steel Plant Tracker.

(a) Pig Iron

(b) DRI

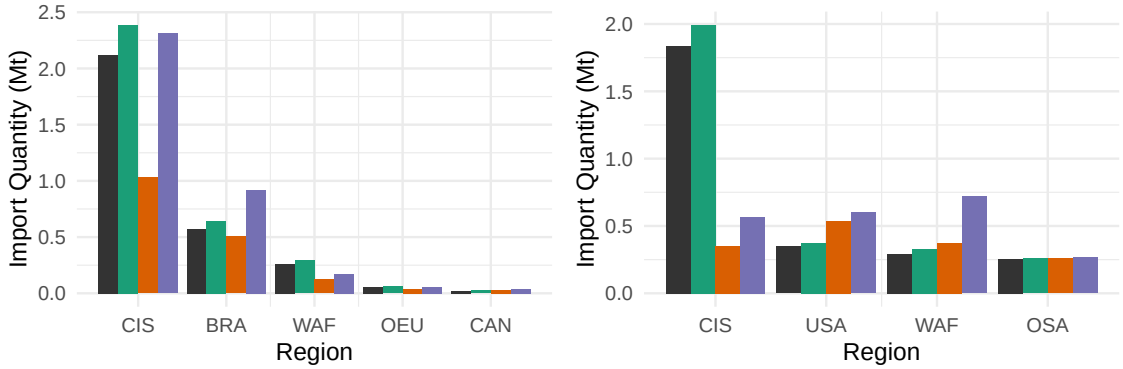

(c) Flat Steel

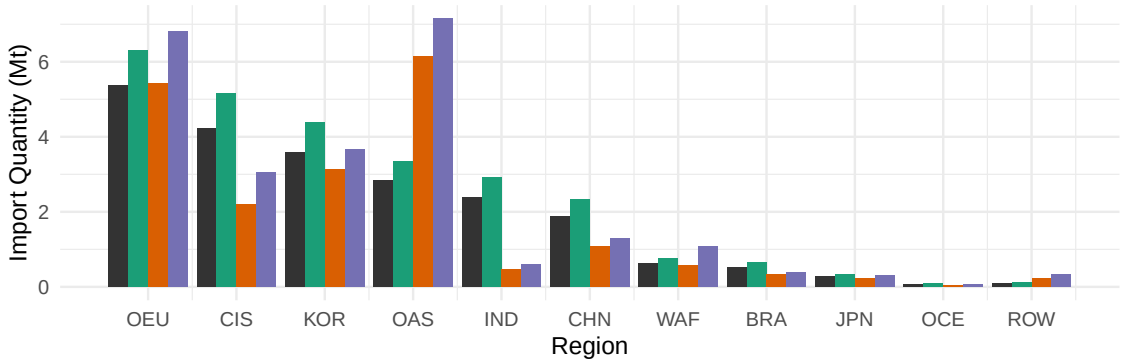

(d) Long Steel

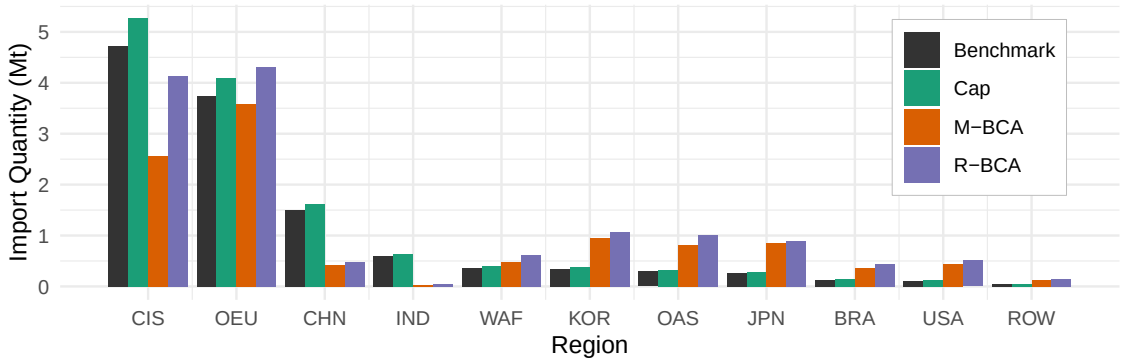

Figure C2. Import Quantity Changes by Product and Exporting Region

Notes: Each panel illustrates the change in import quantities to the EU market for a specific steel product category under the mass-based (M-BCA) and rate-based (R-BCA) scenarios. The data is disaggregated by exporting region, highlighting the differential impacts of the two policy designs on trade flows. Region codes: EU28/EFTA (EUR), US (USA), China (CHN), India (IND), Japan (JPN), South Korea (KOR), Other Asia (OAS), Oceania (OCE), Canada (CAN), Mexico (MEX), Brazil (BRA), Other South America (OSA), Turkey and Other Europe (OEU), CIS and Ukraine (CIS), and Western Asia and Africa (WAF).

Table C1. Calibrated Parameters

Panel (a): Production Substitutions and Transformations

Symbol	Description	Value
Steel Production		
σ_a	Top-level	0.1
σ_a^{KLE}	KLE nest	0.4 (BF/DRF), 0.5 (BOF/EAF)
σ_a^{VA}	Value-added nest	1.0
σ_a^{Ene}	Energy nest	0.1 (BF/DRF), 0.2 (BOF/EAF)
σ_a^{Mat}	Material nest	0.3 (BOF), 0.4 (BF/DRF), 2.5 (EAF)
τ_a	Transformation	0.5
σ_v^{Iron}	Iron make-or-buy	0.1 (Pig iron), 0.5 (DRI)
Macro Production		
σ^C	Top-level	1.0
$\sigma_{\text{mac}}^{\text{VA}}$	Value-added nest	1.255
$\sigma_{\text{mac}}^{\text{Mat}}$	Material nest	0.3

Panel (b): Trade and Final Demand Elasticities

Commodity	Domestic vs. Imported (σ^A)	Across Foreign Origins (σ^M)	Within Domestic (σ^D)
Flat steel	1.4	5.0	5.0
Long steel	1.4	8.0	8.0
Pig iron	1.4	10.0	10.0
DRI	1.4	10.0	10.0
Iron ore	0.9	1.8	–
Steel scrap	2.95	5.9	–
Coal	3.05	6.1	–
Natural gas	10.0	20.0	–
Macro good	2.46	4.92	–

Panel (c): Factor Supply and Mobility Elasticities

Factor (f)	Factor Supply (η_f)	Plant Mobility (η_f^F)
Capital	–	0.1
Labor	–	2.0
Natural gas	2.0	2.9
Electricity	4.0	4.2
Iron ore	10.0	4.5
Coal	10.0	5.8
Steel scrap	0.5	13.8

Table C2. Global Steel Market Structure and Concentration (2015–2019)

		2015		2017		2019	
Company	Headquarter	Prod. (Mt)	Share (%)	Prod. (Mt)	Share (%)	Prod. (Mt)	Share (%)
ArcelorMittal	Luxembourg	97.14	5.98	97.03	5.59	97.31	5.18
China Baowu Group	China	76.40	4.70	65.39	3.76	95.47	5.09
Nippon Steel Corporation	Japan	46.37	2.85	47.36	2.73	51.68	2.75
HBIS Group	China	47.75	2.94	45.56	2.62	46.56	2.48
POSCO	South Korea	41.97	2.58	42.19	2.43	43.12	2.30
Shagang Group	China	34.21	2.11	38.35	2.21	41.10	2.19
Ansteel Group	China	32.50	2.00	35.76	2.06	39.20	2.09
Jianlong Group	China	15.14	0.93	20.26	1.17	31.19	1.66
Tata Steel Group	India	26.31	1.62	25.11	1.45	30.15	1.61
Shougang Group	China	28.55	1.76	27.63	1.59	29.34	1.56
Shandong Steel Group	China	21.69	1.34	21.68	1.25	27.58	1.47
JFE Steel Corporation	Japan	29.83	1.84	30.15	1.74	27.35	1.46
Valin Group	China	14.87	0.92	20.15	1.16	24.31	1.30
Nucor Corporation	United States	19.62	1.21	24.39	1.40	23.09	1.23
Hyundai Steel	South Korea	20.48	1.26	21.23	1.22	21.56	1.15
IMIDRO	Iran	14.10	0.87	15.60	0.90	16.79	0.89
JSW Steel Limited	India	12.42	0.76	16.06	0.92	16.26	0.87
Benxi Steel	China	14.99	0.92	15.77	0.91	16.18	0.86
SAIL	India	14.34	0.88	14.80	0.85	16.18	0.86
Fangda Steel	China	13.21	0.81	15.11	0.87	15.66	0.83
Novolipetsk Steel	Russia	16.05	0.99	17.08	0.98	15.61	0.83
Baotou Steel	China	11.86	0.73	14.20	0.82	15.46	0.82
China Steel Corporation	Taiwan, China	14.82	0.91	15.33	0.88	15.23	0.81
Techint Group	Argentina	8.40	0.52	11.75	0.68	14.44	0.77
Liuzhou Steel	China	10.83	0.67	12.30	0.71	14.40	0.77
Rizhao Steel	China	14.00	0.86	14.98	0.86	14.20	0.76
United States Steel Corporation	United States	14.52	0.89	14.43	0.83	13.89	0.74
EVRAZ	Russia	14.35	0.88	14.03	0.81	13.81	0.74
CITIC Pacific	China	7.61	0.47	8.77	0.50	13.55	0.72
Gerdau S.A.	Brazil	17.03	1.05	16.50	0.95	13.13	0.70
Jingye Group	China	11.32	0.70	10.41	0.60	12.58	0.67
Magnitogorsk (MMK)	Russia	12.24	0.75	12.86	0.74	12.46	0.66
Shaanxi Steel	China	7.47	0.46	10.24	0.59	12.45	0.66
Sanming Steel	China	9.58	0.59	11.19	0.64	12.40	0.66
thyssenkrupp	Germany	17.34	1.07	13.22	0.76	12.25	0.65
Zenith Steel	China	9.08	0.56	10.36	0.60	11.93	0.64
Severstal	Russia	11.45	0.70	11.65	0.67	11.85	0.63
Tsingshan Holding Group	China					11.40	0.61
Nanjing Steel	China	8.59	0.53	9.85	0.57	10.97	0.58
Taiyuan Steel	China	10.26	0.63	10.50	0.60	10.86	0.58
Anyang Steel	China	10.74	0.66	10.06	0.58	10.54	0.56
Global Production (Mt)		1624.38		1736.82		1877.15	
Production Coverage (%)		52.9		51.2		52.4	
Concentration Ratio (CR4)		16.5		14.7		15.5	
Concentration Ratio (CR10)		28.4		26.2		26.9	
HHI Range		120.4–142.0		104.7–129.3		111.4–138.1	

Note: The table includes steel companies with crude steel production exceeding 10 Mt in 2019, sorted by their 2019 production volume. Columns report absolute production in million tonnes (Mt) and global market share (%). Global production (Mt) is total world production. Production coverage is the combined share of firms on this list compared to the global production. Concentration Ratio (CR4) and (CR10) reflect the market share of the four and ten largest firms, respectively. The Herfindahl-Hirschman index (HHI) range reflects the tracked lower bound and a conservative upper bound for the untracked tail. The lower bound is the sum of the squares of the market shares of the tracked firms on the list. The upper bound is a conservative estimate assuming the remaining market share is distributed among firms each equal in size to the smallest tracked firm.
Source: Own calculations based on World Steel Association (2016, 2018, 2020, 2022).

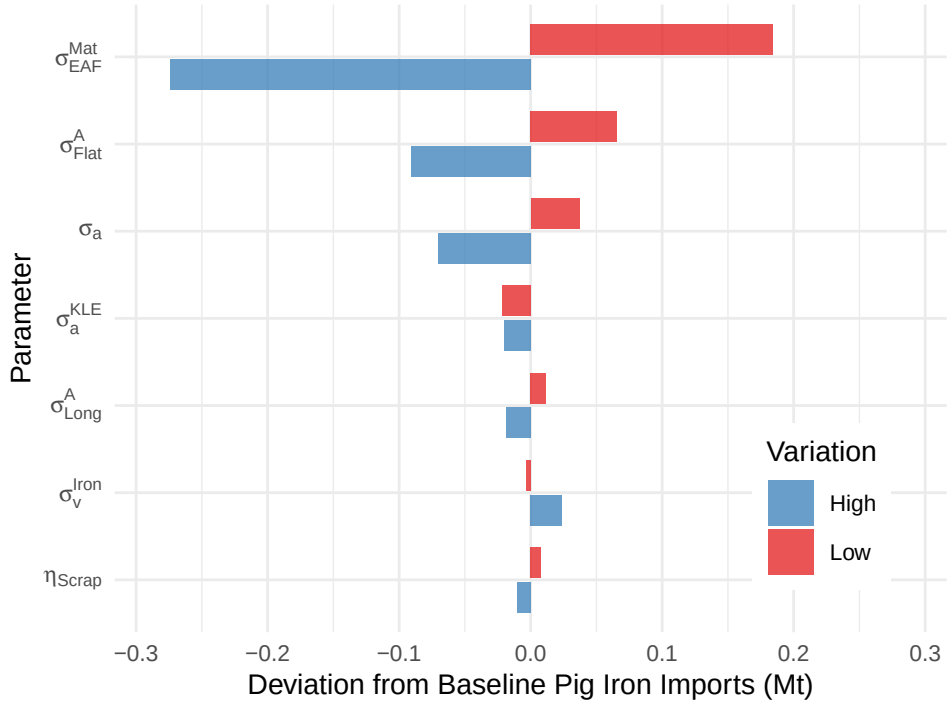

Figure C3. Sensitivity of EU Merchant Pig Iron Imports (Vertical Leakage)

Notes: Bars represent the deviation from the baseline parameter volume of merchant pig iron imports (Mt) into the EU under the EU R-BCA policy design. The horizontal axis indicates the impact of moving each parameter from its calibrated baseline to either its Low (L) or High (H) setting.

Table C3. Market Summary Statistics for EU Scenarios

	Domestic (EUR → EUR)			Import (ROW → EUR)		
Scenario	Quantity	Intensity	Price	Quantity	Intensity	Price
Panel (a): Pig Iron						
Benchmark	4.93	2.12 (0.33)	0.35 (0.04)	3.03	2.67 (0.37)	0.32 (0.03)
Cap	3.50	1.90 (0.27)	0.49 (0.06)	3.41	2.67 (0.36)	0.32 (0.03)
M-BCA	3.45	1.87 (0.26)	0.52 (0.07)	1.73	2.52 (0.32)	0.54 (0.04)
R-BCA	3.51	1.90 (0.26)	0.50 (0.07)	3.50	2.52 (0.31)	0.32 (0.03)
DM-BCA	3.51	1.89 (0.26)	0.50 (0.07)	2.64	2.60 (0.34)	0.39 (0.03)
Panel (b): Long Steel						
Benchmark	60.71	0.58 (0.79)	0.45 (0.04)	12.11	2.07 (1.01)	0.40 (0.07)
Cap	58.54	0.44 (0.61)	0.49 (0.05)	13.32	2.06 (1.01)	0.40 (0.07)
M-BCA	60.47	0.42 (0.58)	0.50 (0.06)	10.59	1.04 (1.05)	0.49 (0.10)
R-BCA	58.88	0.43 (0.60)	0.49 (0.05)	13.65	1.04 (1.01)	0.39 (0.09)
DM-BCA	59.36	0.43 (0.60)	0.50 (0.05)	11.83	1.69 (1.12)	0.44 (0.08)

Notes: Values represent the production-weighted mean and standard deviation (in parentheses) for domestic production (EU) and imports (ROW) across scenarios. Intensity is measured in tCO_2/ton of product. Quantity is measured in Mt. Price represents the delivered price in 1000 USD/ton.

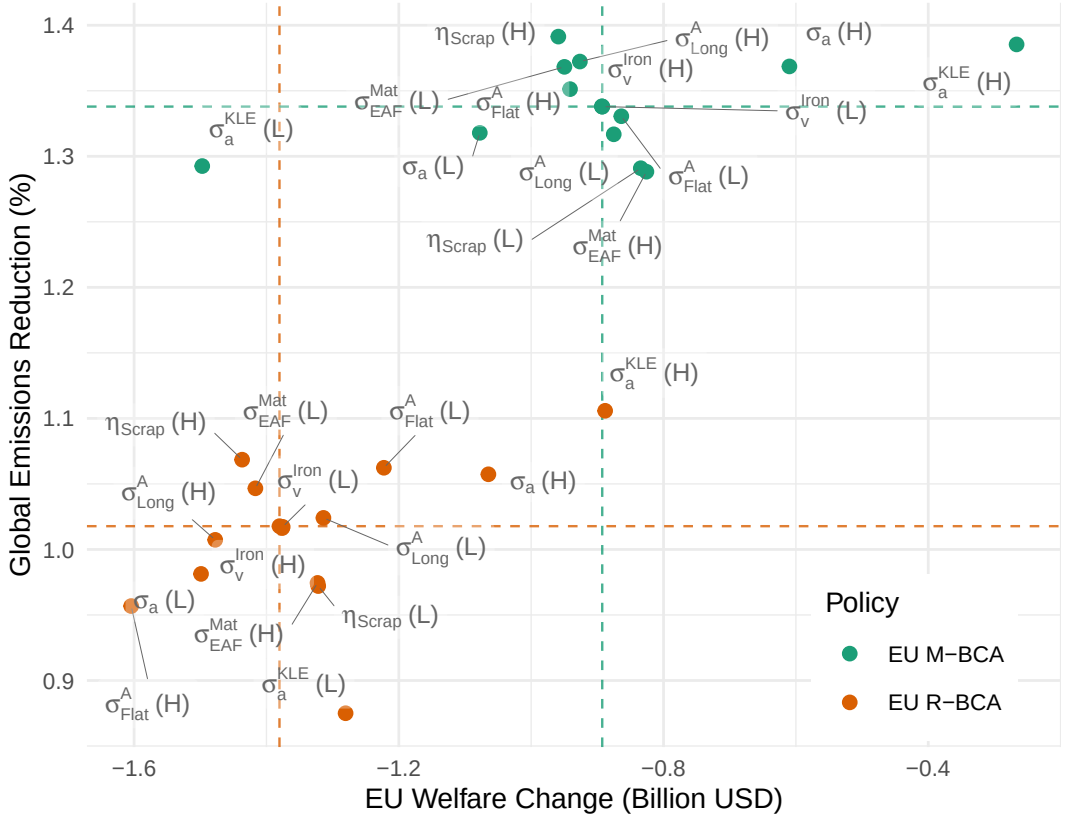

Figure C4. Sensitivity of Global Cost-Effectiveness Frontier

Notes: The scatter plot maps global emissions reduction against regional welfare for all 28 sensitivity scenarios across two EU policy designs. Dashed lines mark the baseline parameter cost-effectiveness coordinates for the EU M-BCA and EU R-BCA. (H) and (L) denote High and Low parameter variations respectively.

Table C4. Reshuffling Index (R) for EU Scenarios

Product	Benchmark	Cap	M-BCA	R-BCA	DM-BCA
Pig Iron	1.02	1.02	0.96	0.96	1.00
DRI	0.70	0.70	0.66	0.66	0.69
Flat Steel	0.85	0.86	0.53	0.53	0.74
Long Steel	1.08	1.09	0.55	0.55	0.90

Notes: The Reshuffling Index (R) is defined as the ratio of the emissions intensity of exports to the regulating region relative to the producer's domestic average intensity ($R = e_{exp}/e_{dom}$). Values less than 1 indicate that the producer is exporting cleaner-than-average output to the regulating region, while values greater than 1 indicate that dirtier-than-average output is being exported. The table compares R under EU scenarios.

Table C5. Robustness of Policy Efficiency

Param.	Var.	EU M-BCA		EU R-BCA		US M-BCA		US R-BCA	
		Welf. ($bn)	Red. (%)	Welf. ($bn)	Red. (%)	Welf. ($bn)	Red. (%)	Welf. ($bn)	Red. (%)
Baseline	Base	-0.89	1.34	-1.38	1.02	-0.87	0.26	-0.32	0.06
σ_v^{Iron}	Low	-0.89	1.34	-1.38	1.02	-0.88	0.26	-0.32	0.06
σ_v^{Iron}	High	-0.89	1.34	-1.38	1.02	-0.88	0.26	-0.32	0.06
η_{Scrap}	Low	-0.83	1.29	-1.32	0.97	-0.88	0.24	-0.31	0.06
η_{Scrap}	High	-0.96	1.39	-1.44	1.07	-0.86	0.28	-0.32	0.07
σ^A_{Flat}	Low	-0.86	1.33	-1.22	1.06	-0.75	0.25	-0.31	0.06
σ^A_{Flat}	High	-0.94	1.35	-1.60	0.96	-1.07	0.28	-0.34	0.07
σ^A_{Long}	Low	-0.88	1.32	-1.31	1.02	-0.85	0.26	-0.31	0.06
σ^A_{Long}	High	-0.93	1.37	-1.48	1.01	-0.92	0.26	-0.33	0.07
$\sigma^{\text{Mat}}_{\text{EAF}}$	Low	-0.95	1.37	-1.42	1.05	-0.68	0.22	-0.32	0.07
$\sigma^{\text{Mat}}_{\text{EAF}}$	High	-0.83	1.29	-1.32	0.97	-1.09	0.29	-0.33	0.06
σ_a^{KLE}	Low	-1.50	1.29	-1.28	0.87	-0.61	0.23	-0.21	0.05
σ_a^{KLE}	High	-0.27	1.39	-0.89	1.11	-0.74	0.26	-0.26	0.06
σ_a	Low	-1.08	1.32	-1.50	0.98	-0.90	0.26	-0.32	0.06
σ_a	High	-0.61	1.37	-1.06	1.06	-0.73	0.24	-0.26	0.06

Notes: Results report regional welfare change (billion USD) and global emissions reduction (%) relative to the no-policy equilibrium. Scenarios are evaluated at a fixed stringency of a 30% reduction in domestic emissions for the EU. Parameters are varied by a factor of 0.5 (L) or 2.0 (H) relative to calibrated values, except for σ_v^{Iron} which uses a 5.0 factor for High (H) elasticity.

Table C6. Sensitivity of Leakage and Protection

Param.	Var.	EU M-BCA		EU R-BCA		US M-BCA	US R-BCA
		Leak. (%)	Pig I. (Mt)	Leak. (%)	Pig I. (Mt)	Rev. Lk. (%)	Rev. Lk. (%)
Baseline	Base	16.0	1.73	36.1	3.50	23.0	14.9
σ_v^{Iron}	Low	16.0	1.73	36.2	3.49	23.0	14.9
σ_v^{Iron}	High	16.0	1.72	36.2	3.52	23.1	14.9
η_{Scrap}	Low	19.0	1.73	39.0	3.50	24.8	16.5
η_{Scrap}	High	12.7	1.73	33.0	3.49	21.3	13.3
σ^A_{Flat}	Low	16.5	1.73	33.3	3.56	15.2	9.5
σ^A_{Flat}	High	15.2	1.72	40.0	3.41	31.8	23.4
σ^A_{Long}	Low	17.4	1.73	35.7	3.51	22.2	13.0
σ^A_{Long}	High	13.9	1.74	36.8	3.48	24.3	17.8
$\sigma^{\text{Mat}}_{\text{EAF}}$	Low	14.1	1.89	34.3	3.68	31.4	14.9
$\sigma^{\text{Mat}}_{\text{EAF}}$	High	19.2	1.54	38.9	3.22	14.7	15.1
σ_a^{KLE}	Low	18.9	1.58	45.1	3.47	21.5	12.6
σ_a^{KLE}	High	13.1	1.95	30.6	3.48	22.1	12.6
σ_a	Low	17.3	1.70	38.4	3.53	22.1	15.0
σ_a	High	14.1	1.79	33.7	3.43	24.0	13.3

Notes: Leak. refers to the global leakage rate for the EU scenarios. Pig I. refers to the volume of merchant pig iron imports into the EU (Mt). Rev. Lk. refers to reverse leakage (onshoring) in the US scenarios.

Table C7. Abatement Margins in the ROW (EU R-BCA)

Param.	Var.	Scale (Mt)	Composition (Mt)	Technique (Mt)	Total (Mt)
Baseline	Base	37.77	-3.71	2.96	37.02
σ_v^{Iron}	Low	37.81	-3.70	2.96	37.07
σ_v^{Iron}	High	37.81	-3.70	2.97	37.08
η_{Scrap}	Low	38.84	-2.51	4.22	40.55
η_{Scrap}	High	36.64	-5.06	1.53	33.11
σ^A_{Flat}	Low	34.95	-3.98	2.99	33.97
σ^A_{Flat}	High	41.70	-3.41	2.90	41.19
σ^A_{Long}	Low	37.41	-3.64	2.95	36.72
σ^A_{Long}	High	38.37	-3.81	2.98	37.54
$\sigma^{\text{Mat}}_{\text{EAF}}$	Low	36.69	-3.50	1.93	35.11
$\sigma^{\text{Mat}}_{\text{EAF}}$	High	39.35	-3.99	4.41	39.76
σ_a^{KLE}	Low	47.65	-1.80	2.60	48.45
σ_a^{KLE}	High	30.78	-3.48	3.64	30.94
σ_a	Low	40.23	-3.61	2.98	39.61
σ_a	High	34.73	-3.23	3.14	34.64

Notes: The table decomposes the rest of the world (ROW) emissions response (Mt CO_2) for the intensity-based design into scale, composition, and technique effects using an LMDI decomposition. Scale represents production volume shifts; Composition represents shifts between primary and secondary routes; Technique represents within-technology efficiency gains.